NUMERICAL SOLUTION FOR STRATIFIED LAMINAR FLOW OF TWO IMMISCIBLE NEWTONIAN LIQUIDS IN A CIRCULAR PIPE

by

ALAN ROBERT GEMMELL

B.A.Sc., University of Toronto, 1959

A THESIS SUBMITTED IN PARTIAL FULFILMENT OF THE REQUIREMENTS FOR THE DEGREE OF

MASTER OF APPLIED SCIENCE

in the Department

of

CHEMICAL ENGINEERING

We accept this thesis as conforming to the required standard

Members of the Department of
Chemical Engineering

THE UNIVERSITY OF BRITISH COLUMBIA

January 1961

In presenting this thesis in partial fulfilment of the requirements for an advanced degree at the University of British Columbia, I agree that the Library shall make it freely available for reference and study. I further agree that permission for extensive copying of this thesis for scholarly purposes may be granted by the Head of my Department or by his representatives. It is understood that copying or publication of this thesis for financial gain shall not be allowed without my written permission.

Department of CHEMICAL ENGINEERING

The University of British Columbia,
Vancouver 8, Canada.

Date FEB. 11, 1961

ABSTRACT

Numerical solutions of the velocity profiles for laminar, stratified flow of two immiscible, Newtonian liquids in a circular pipe were determined for viscosity ratios of 1, 10, 100 and 1000 at various interface positions. These results were used to calculate the theoretical volumetric flow rate enhancement factors, power reduction factors and hold-up ratios, which for laminar flow depend only upon the viscosity ratio and the interface position. The maximum volumetric flow rate enhancement factors and maximum power reduction factors, and the corresponding input volume ratios, were determined. Dimensionless quantities were used, making the results applicable to any pipe diameter, any liquid viscosities and any pressure gradient, providing laminar flow of both phases prevails.

The theoretical results were compared to the experimental results of Russell, Hodgson and Govier for horizontal cocurrent flow of a mineral oil and water in a circular pipe. As expected, the two sets of results differed considerably in the region of turbulent water flow. As turbulence decreased however, the difference decreased, until in the laminar region very good agreement between the theoretical and experimental results was obtained.

ACKNOWLEDGEMENTS

I wish to thank Dr. Norman Epstein, under whose direction this investigation was conducted, for his excellent guidance and continued assistance throughout the study.

I am also indebted to the Standard Oil Company of British Columbia Limited for financial assistance received in the form of their graduate Fellowship, and the National Research Council of Canada for additional support.

TABLE OF CONTENTS

LIST OF FIGURES

Figure

Page

LIST OF TABLES

NOMENCLATURE

a - constant in polynomial equation

b - constant in polynomial equation

c - constant in polynomial equation

d - constant in polynomial equation

D - diameter of pipe

e - constant in polynomial equation

f - external force

g_c - gravitational constant

h - distance between equally spaced points in Douglass-Avakian method

k - coefficient of h

L - length of pipe

p - distance from interior nodal point to the boundary

P - pressure

ΔP - frictional pressure drop

q - distance from external nodal point to the boundary

Q - volumetric flow rate

r - radial distance from centre of the pipe

R - radius of pipe

Re - Reynolds number

s - half the distance between infinite parallel plates

t - time

u - velocity in the x direction

u' - dimensionless velocity, $\frac{u}{U}$, in x direction

U - average velocity in x direction

v - velocity in the y direction

V - superficial velocity

w - velocity in the z direction

W - power per unit length

x - Cartesian coordinate; horizontal distance along the length of the pipe

x' - $\frac{x}{R}$, dimensionless

X - variable in polynomial equation

y - Cartesian coordinate; vertical distance from bottom of the pipe

y' - $\frac{y}{R}$, dimensionless

Y - variable in polynomial equation

z - Cartesian coordinate; horizontal distance across the pipe

z' - $\frac{z}{R}$, dimensionless

Z - variable in polynomial equations, $Z = Y - 3h$

Δ - incremental quantity

Σ - sum

μ - viscosity

μ' - viscosity ratio = μ_A/μ_B

π - 3.1416

ρ - density

Θ - central angle of sector, radians

Subscripts

A - more viscous liquid

B - less viscous liquid

full - indicates pipe flowing full of liquid A

i - interface

m - horizontal coordinate of relaxation grid

n - vertical coordinate of relaxation grid

0,1,2,3,4 - points in relaxation pattern

w - water

INTRODUCTION

The pipeline transportation of heavy crude oil is difficult because of the high viscosity of the oil. Large and closely-spaced pumping stations are required to overcome the high frictional pressure drop associated with very viscous oil. It has been found (1,2,3,4,6) that addition of water to the oil decreases the resistance to flow and for certain proportions of water, the same volumetric flow rate of oil can be maintained at lower pressure gradients and lower power requirements.

Clarke (1), in a private communication to Russell and Charles (2), reported results using a heavy viscous crude oil flowing in a 0.375-inch pilot pipeline at Reynolds numbers of 10 to 20. The pressure gradient was reduced by factors of 6 to 12 when 7-13% water was introduced. The shape of the interface was not known but "it was suggested that the water wetted the inside of the pipe preferentially."

Clark and Shapiro (3) patented a method, described by Russell and Charles (2), whereby they injected water and demulsifying agents into the flowing crude oil. Using oils of viscosities estimated at 800 to 1000 cp., results were reported for laminar flow in a 6-inch commercial pipeline

3 miles long. They observed pressure gradient reduction factors ranging from 7.8 to 10.5 with the injection of 7-24 % water, and the maximum reduction factor at a water input of 8-10%.

Chilton and Handley (4) patented a process in 1958 which was subsequently mentioned in a letter by Chilton (5). They observed a pressure drop reduction by adding a film of water at the wall of a pipe carrying extremely highly viscous crude oil. Over a 50-foot length of approximately one-inch pipeline there appeared no mixing of the oil and water, and the water film remained essentially intact over this distance.

Russell, Hodgson, and Govier (6) studied stratified flow of a refined mineral oil and water in a 28-foot transparent pipeline with a 0.806-inch diameter. The oil, which had a viscosity of 18 cp., was observed to be flowing above the water in the laminar region. At a water content of 10%, the pressure gradient was reduced by a factor of 1.2 at Reynolds numbers of 10 to 400. The authors also found that hold-up ratio was a function of the input volume ratio in the laminar region, and was also a function of velocity of the liquids in the turbulent region.

The experimental results discussed above are

summarized in Table I as in Russell and Charles (2). While the maximum pressure gradient reduction factor for an oil of viscosity 18 cp. was listed as 1.2, which corresponds to 10% by volume of water input, examination of the actual data of Russell, Hodgson and Govier (6,7) showed factors as high as 1.52, which occurred at approximately 40% water input.

The existence of an interface between the oil and the water is substantiated by the findings of Tipman and Hodgson (8) and Pavlov (9) as discussed by Russell and Charles(2). The former investigators found that the viscosity of an oil and water emulsion is almost always greater than that of the pure oil. Therefore Russell and Charles concluded that a pressure gradient reduction can only occur if the water flows as a separate phase.

Two flow models for stratified laminar flow of two immiscible liquids were investigated theoretically by Russell and Charles (2). The first model studied was that of a more viscous liquid, A, flowing above a less viscous liquid, B, between infinite parallel plates. Equations relating pressure drop to geometry, flow rates and viscosities were developed. This was done by applying force balances to the two liquids and assuming that the velocities of the two are equal at the interface, which results in expressions for the volumetric flow rates of the more

TABLE I

PREDICTED AND OBSERVED PRESSURE GRADIENT REDUCTION FACTORS FOR OIL-WATER FLOW (2)

Reference	Oil Type	Oil gravity, °API	Oil viscosity, cp.	Maximum predicted gradient reduction factor		Maximum observed pressure gradient reduction factor
				Concentric flow	Parallel plates	
Clarke(1)	Crude	7.0	800-1000*	400-500	3-4	12
Clark and Shapiro (3)	Crude	13.4	800-1000**	400-500	3-4	10.5
Russell et al (6)	Refined	38	18	9	2.2	1.2

* Estimated viscosity of McMurray oil-sand oil at 70°C., the temperature at which the observations were made.

** Estimated from a general knowledge of the viscosity of heavy crude oils at normal pipeline temperatures.

viscous liquid, Q_A, and the less viscous liquid, Q_B. The minimum frictional pressure gradient was found by differentiating the expression for $Q_A/(\frac{\Delta P}{\Delta L})$ with respect to the interfacial position, and equating the result to zero. Optimum positions of the interface for the greatest reduction in the pressure gradient were determined for viscosity ratios greater than one. As reported in Table I, the maximum pressure gradient reduction factor is 4 for an oil of viscosity 1000 cp. and 2.2 for an oil of viscosity 18 cp., flowing with water between parallel plates. It was also shown that the minimum power requirement could be computed by differentiating the expression for $\frac{\Delta P}{\Delta L}(Q_A + Q_B)$ with respect to interfacial position and equating the result to zero.

The second model studied was that of concentric flow of two immiscible liquids in a circular pipe. The less viscous liquid flowed next to the pipe wall as an annulus, with the more viscous liquid flowing inside of it. Force balances were again employed to obtain expressions for the volumetric flow rates of the two liquids. By differentiating the expression for $Q_A/(\frac{\Delta P}{\Delta L})$ with respect to the interfacial position and equating the result to zero, an interfacial position was determined for the maximum pressure gradient reduction. As before, optimum positions were found for viscosity ratios greater than one. Expressions were also obtained for maximum pressure gradient reduction factors,

by comparing the pressure drop for two-phase flow to the pressure drop if the pipe were flowing full of the more viscous liquid at its same volumetric flow rate. The pressure gradient reduction factors for concentric flow are very much greater than those obtained for parallel plate flow, as is shown in Table I. For an oil of viscosity 1000 cp., the maximum pressure gradient reduction factor is 500 and for a viscosity of 18 cp., it is 9. Power reduction factors were determined in a manner similar to that of determining pressure gradient reduction factors. The position of the interface for maximum power reduction factor was closer to the wall of the pipe than the interface position for maximum pressure gradient reduction factor.

The results, summarized in Table I, show that those values derived from the two theoretical models are quite different from each other and also quite different from the available field data. Maximum pressure gradient reduction factors determined experimentally for the two crude oils fall between the values predicted by the two theoretical models. However, the values of the maximum factor measured for the refined oil, which was observed to be flowing as a stratified layer, fell below those predicted by the theoretical models. Russell and Charles concluded that for stratified flow in a circular pipe, the maximum pressure gradient reduction factor falls below that

predicted for parallel plate flow. Since the measured values for the crude oils were 10.5 and 12, which are above the 3-4 predicted for parallel plate flow, they concluded that in these cases the flow must be intermediate between concentric and stratified flow. It is thought that such a conclusion cannot be drawn, because of the absence of the theoretical solution for stratified flow in a circular pipe and because of the sparseness of the available experimental data.

The purpose of the present study was to provide the theoretical solution for the case of stratified laminar flow of two immiscible Newtonian liquids in a circular pipe. The results of this investigation could then be used to predict pressure gradient and power reduction factors for this type of flow as well as hold-up and optimum input ratios. Also, the added results could be used to either substantiate or dispute the above conclusion of Russell and Charles. The two liquids involved do not necessarily have to be oil and water but can be any two immiscible liquids, and therefore the model was solved for viscosity ratios, rather than absolute viscosities, of 1.0, 10, 100 and 1000. The cases of viscosity ratios of 10, 100 and 1000 were solved for 8 different interface positions. Dimensionless flow equations were solved numerically, using relaxation methods, to obtain velocity profiles for any size of pipe. Volumetric flow rates were easily determined from the velocity

profiles. From these data, values of the pressure gradient reduction factors and power reduction factors were determined as well as location of the interface for the maximum factors. The relationship between hold-up ratio, input volume ratio and viscosity ratio were also shown.

The theoretical results were compared to the experimental case of stratified flow (6) for a viscosity ratio of 20.1, with regards to hold-up ratios, frictional pressure drop and pressure gradient reduction factors.

COMPUTATIONS

A. Velocity Profiles

a. Theory

The present study considers the stratified, laminar flow of two immiscible, incompressible, Newtonian liquids in a circular pipe. A schematic diagram of the flow situation is shown in figure 1 with the coordinate axis marked.

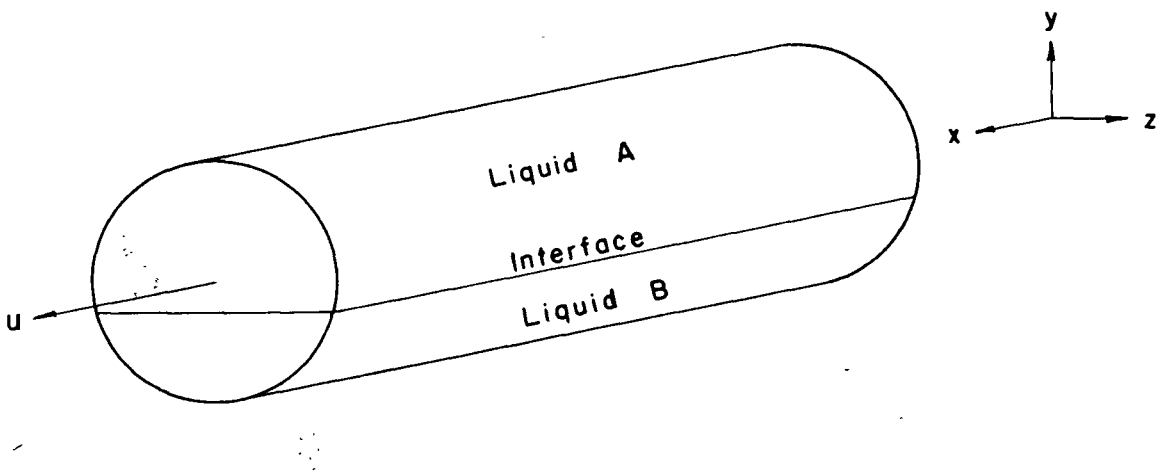

Figure 1. Schematic Diagram of Flow Model
(liquid B more dense than liquid A)

The basic assumption is made that the velocity at the pipe wall is zero. It is further assumed that at the interface both liquids display the same velocities and equal but opposite shear stresses with respect to the

interface. These boundary conditions can be applied to the Navier-Stokes momentum equations, which describe the flow.

The Navier-Stokes equation for an incompressible fluid flowing in the x direction is expressed as

$$\frac{Du}{Dt} = u\frac{\partial u}{\partial x} + v\frac{\partial u}{\partial y} + w\frac{\partial u}{\partial z} + \frac{\partial u}{\partial t} = f_x - \frac{1}{\rho}\frac{\partial P}{\partial x} + \frac{\mu}{\rho}\left(\frac{\partial^2 u}{\partial x^2}+\frac{\partial^2 u}{\partial y^2}+\frac{\partial^2 u}{\partial z^2}\right) \quad (1)$$

Because laminar, stratified flow is assumed in a conduit of constant cross-sectional area, there is no flow in the y and z directions and the Navier-Stokes equations vanish for these two coordinate directions.

The continuity equation for steady-state flow of an incompressible fluid is

$$\frac{\partial u}{\partial x} + \frac{\partial v}{\partial y} + \frac{\partial w}{\partial z} = 0 \quad (2)$$

Because there is flow only in the x direction, v = 0 and w = 0 and therefore

$$\frac{\partial u}{\partial x} = 0 \quad (3)$$

Also since steady-state exists,

$$\frac{\partial u}{\partial t} = 0 \quad (4)$$

and therefore

$$\frac{Du}{Dt} = 0 \quad (5)$$

From equation (3) it follows that

$$\frac{\partial^2 u}{\partial x^2} = 0 \tag{6}$$

As there are no significant external forces in the x direction,

$$f_x = 0 \tag{7}$$

The Navier-Stokes momentum equations thus reduce to the following single equation for the case of steady-state, laminar flow of an incompressible liquid in the x direction:

$$\frac{\partial P}{\partial x} = \mu \left(\frac{\partial^2 u}{\partial y^2} + \frac{\partial^2 u}{\partial z^2}\right) \tag{8}$$

Equation (8) applies to each liquid, using its respective viscosity.

At the interface, the condition of equal and opposite shear stresses is expressed as

$$\mu_A \frac{\partial u_A}{\partial y} = \mu_B \frac{\partial u_B}{\partial y} \tag{9}$$

Equations (8) and (9) restricted by the requirement of no slip at the wall and at the interface describe completely the flow conditions investigated.

The absolute quantities of these equations are transformed to dimensionless quantities, so that the results are applicable to any pressure gradient, pipe diameter and

viscosity ratio of the two phases, rather than to specific pressure gradients, pipe diameters and viscosities. This is achieved by letting:

$$u' = \frac{u}{U_A} \tag{10}$$

where $$U_A = \frac{R^2}{8\mu_A} \left(- \frac{\partial P}{\partial x} \right) \tag{11}$$

The quantity U_A is the average velocity in a pipe flowing full of liquid A at the same pressure gradient as in the two-phase flow. The following dimensionless distances are used:

$$y' = \frac{y}{R}, \qquad z' = \frac{z}{R} \tag{12}$$

Substitution of equations (10), (11) and (12) into equations (8) and (9) converts the Navier-Stokes equation to

$$\frac{\partial^2 u'}{\partial y'^2} + \frac{\partial^2 u'}{\partial z'^2} = - 8 \frac{\mu_A}{\mu} \tag{13}$$

and the shear force equation to

$$\frac{\mu_A}{\mu_B} \frac{\partial u'_A}{\partial y'} = \frac{\partial u'_B}{\partial y'} \tag{14}$$

The finite difference approximation of equation (13) as shown in Mickley, Sherwood and Reed (10), is expressed as

$$\frac{u'_{m-1,n} - 2u'_{m,n} + u'_{m+1,n}}{(\Delta y')^2} + \frac{u'_{m,n-1} - 2u'_{m,n} + u'_{m,n+1}}{(\Delta z')^2} = - 8 \frac{\mu_A}{\mu} \tag{15}$$

The relaxation pattern, as shown in figure 2, is obtained by letting $\Delta y' = \Delta z'$ and substituting subscripts 1,2,3 and 4 for m,n-1, m+1,n, m,n+1 and m-1,n respectively. These four points are situated on straight lines at right angles to each other and at equal distances from the central point O, which is substituted for m,n.

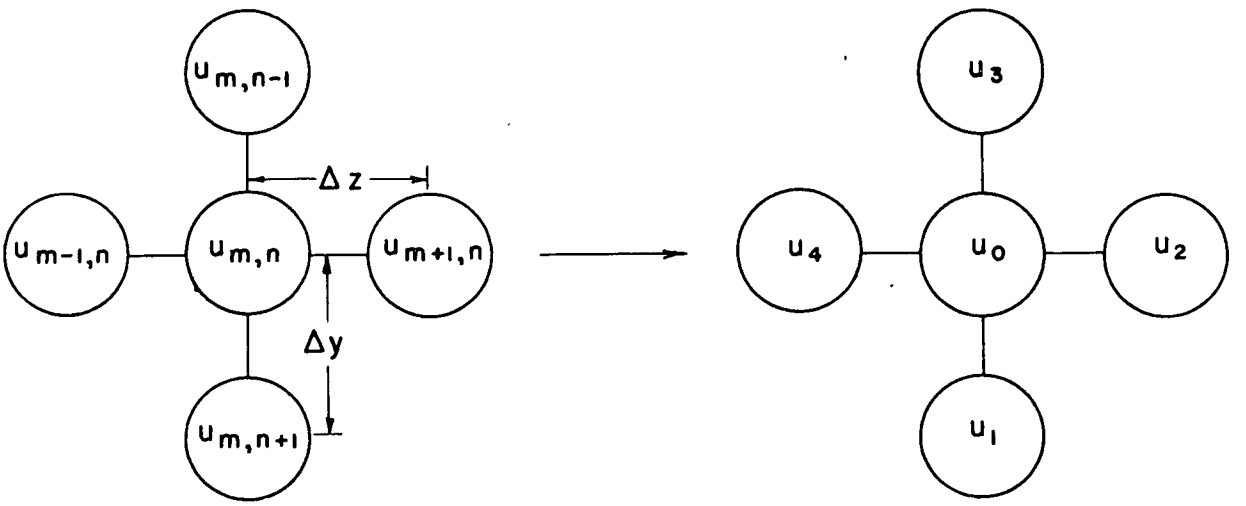

Figure 2. Relaxation Pattern

Equation (15) then simplifies to

$$u'_1 + u'_2 + u'_3 + u'_4 - 4u'_o + 8\frac{\mu_A}{\mu}(\Delta y')^2 = 0 \qquad (16)$$

which is the general numerical flow equation to be applied to each liquid. This equation is solved by relaxation methods which are described briefly in Appendix I.

The general procedure for obtaining a numerical equation applicable at the interface is found in Allen (11), and was followed in this study. The finite difference approximation to equation (14) is

$$\frac{\mu_A}{\mu_B}\,(u'_{A_1}-u'_{A_3}) = (u'_{B_1}-u'_{B_3}) \qquad (17)$$

By examining the relaxation pattern at the interface, as in figure 3 below, it is seen that the velocities u'_{A_1} and u'_{B_3} are fictitious because u'_{A_1} is in liquid B and u'_{B_3} is in liquid A.

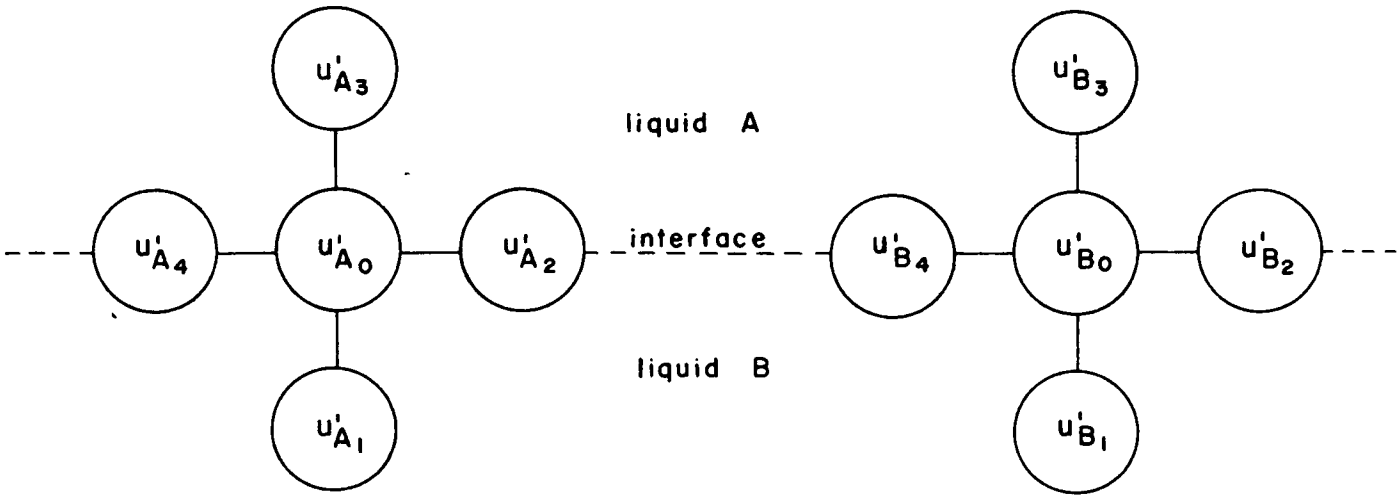

Figure 3. Relaxation Patterns at the Interface

Therefore u'_{A_1} and u'_{B_3} must be eliminated by substitution.

Rewriting equation (16) as it applies to each liquid, A and B, and letting $\frac{\mu_A}{\mu_B} = \mu'$, a dimensionless viscosity ratio, the following two equations result:

$$u'_{A_1} + u'_{A_2} + u'_{A_3} + u'_{A_4} - 4u'_{A_o} + 8(\Delta y')^2 = 0 \quad (18)$$

$$u'_{B_1} + u'_{B_2} + u'_{B_3} + u'_{B_4} - 4u'_{B_o} + 8\mu'(\Delta y')^2 = 0 \quad (19)$$

Multiplying equation (18) by μ' and subtracting equation (17) from it eliminates u'_{A_1}. Subtraction of equation (19) from the resulting equation, eliminates u'_{B_3}. Since the velocities at the interface are assumed equal, $u'_{A_o} = u'_{B_o}$, $u'_{A_2} = u'_{B_2}$ and $u'_{A_4} = u'_{B_4}$, and therefore the final equation at the interface is

$$\frac{2}{\mu'+1} u'_{B_1} + u'_{A_2} + \frac{2\mu'}{\mu'+1} u'_{A_3} + u'_{A_4} - 4u'_{A_o} + \frac{16\mu'}{\mu'+1}(\Delta y')^2 = 0 \quad (20)$$

Equations (18) and (19) in the main body of each liquid, respectively, equation (20) at the interface, and no slip at the wall fully describe the flow conditions. These equations were solved by relaxation methods to obtain point velocities throughout a relaxation grid for viscosity ratios of 10,100 and 1000 at 8 different interface positions. Points of the grid which were outside the curved boundary, on which all velocities are zero, were assigned negative values by extrapolating linearly as in figure 4.

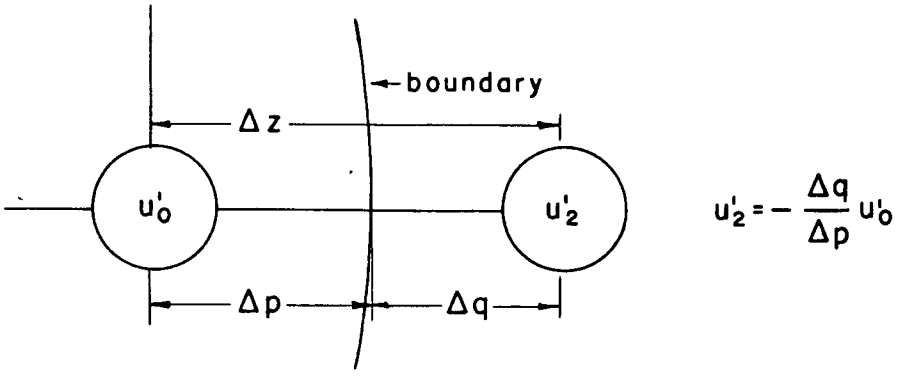

Figure 4. Boundary Conditions

In the case of a viscosity ratio of one, the two liquids flow as one, that is, without any discontinuity in the rate of shear. Therefore the same velocity profile exists for all interface positions. The grid point velocities were calculated by relaxation methods and from the Poiseuille equation,

$$u = \frac{(R^2-r^2)}{4\mu} \left(-\frac{\partial P}{\partial x}\right) \tag{22}$$

$$U = \frac{R^2}{8\mu} \left(-\frac{\partial P}{\partial x}\right) \tag{11}$$

Therefore $$u' = \frac{u}{U} = 2\,\frac{(R^2-r^2)}{R^2} \tag{22a}$$

The velocity profile obtained from the Poiseuille equation was used to calculate derivative results for seventeen interface positions.

b. Sample Calculations

Sample calculations are shown for a viscosity ratio of 10 and an interface situated mid-way between the centre and bottom of the pipe. If y is the vertical height of the interface from the bottom of the pipe, this position corresponds to $y_i = \frac{R}{2}$. Each case was solved for three different grid sizes, progressing from a coarse grid to a fine grid, unless a reasonable estimate of the velocities could be made directly for the finer grid.

Initial grid size = $\frac{R}{2}$

Therefore $\Delta y' = \frac{1}{2}$ and $(\Delta y')^2 = \frac{1}{4}$

and the resulting flow equations are

for liquid A: $u'_{A_1} + u'_{A_2} + u'_{A_3} + u'_{A_4} - 4u'_{A_o} + 2.00 = 0$ (18a)

at interface: $0.182u'_{B_1} + u'_{A_2} + 1.82u'_{A_3} + u'_{A_4} - 4u'_{A_o} + 3.64 = 0$ (20a)

and for liquid B: $u'_{B_1} + u'_{B_2} + u'_{B_3} + u'_{B_4} - 4u'_{B_o} + 20.0 = 0$ (19a)

These equations were solved by relaxation methods, typical calculations of which are shown in figure 5. Only half of the pipe cross-section was considered because the velocity profile is symmetrical about the vertical axis through the centre of the pipe. This condition of symmetry was imposed when performing the relaxation about the vertical axis, as illustrated in figure 7.

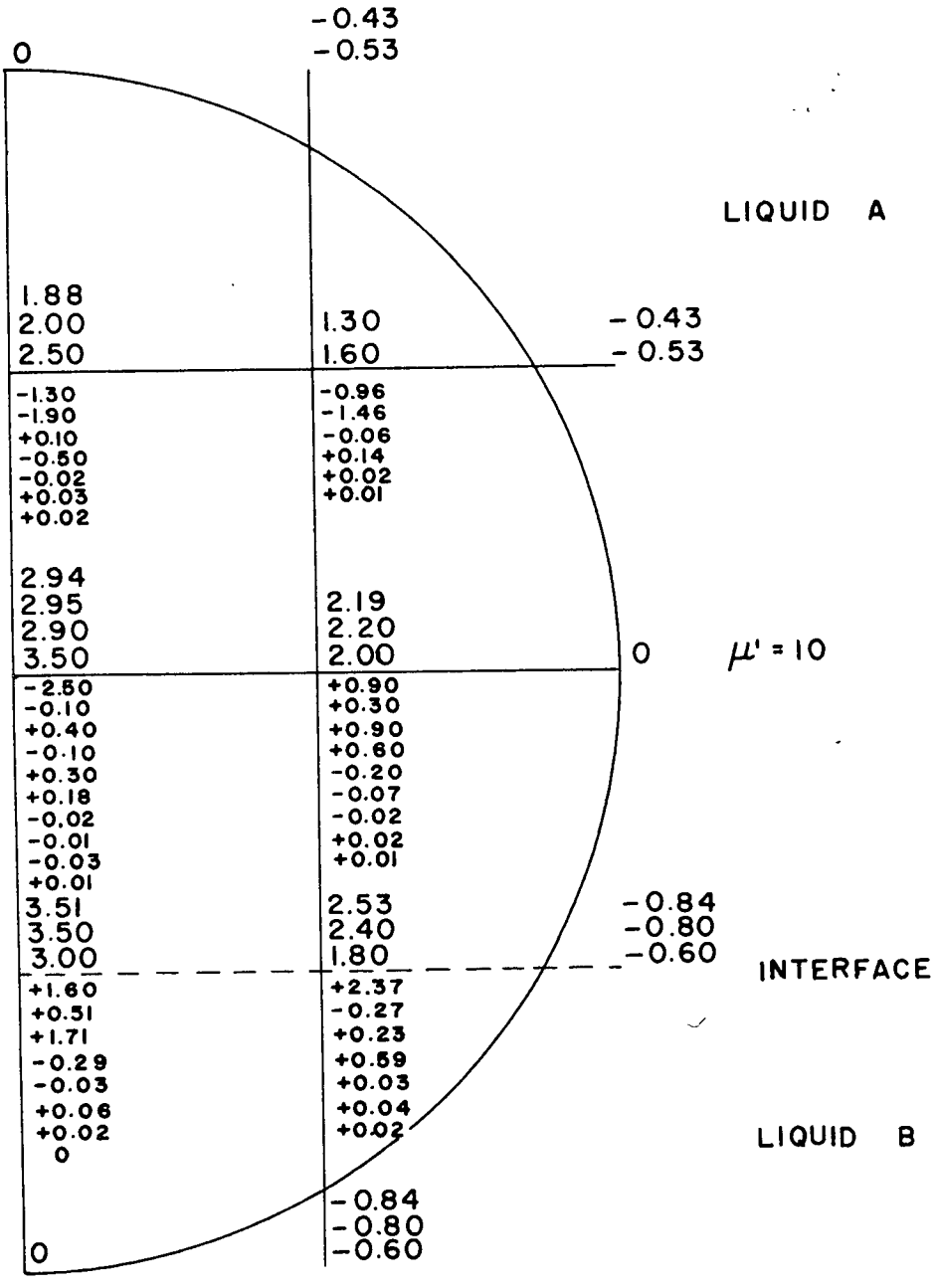

Figure 5. Sample Relaxation Calculations
(small numbers denote residuals)
(large numbers denote values of u')

Intermediate grid size = $\frac{R}{4}$.

Therefore $\Delta y' = \frac{1}{4}$ and $(\Delta y')^2 = \frac{1}{16}$

and the resulting flow equations are

for liquid A: $u'_{A_1} + u'_{A_2} + u'_{A_3} + u'_{A_4} - 4u'_{A_o} + 0.50 = 0$ (18b)

at interface: $0.182u'_{B_1} + u'_{A_2} + 1.82u'_{A_3} + u'_{A_4} - 4u'_{A_o} + 0.91 = 0$ (20b)

and for liquid B: $u'_{B_1} + u'_{B_2} + u'_{B_3} + u'_{B_4} - 4u'_{B_o} + 5.00 = 0$ (19b)

These equations are solved in a similar manner to the equations for the coarser grid.

Final grid size = $\frac{R}{8}$

Therefore $\Delta y' = \frac{1}{8}$ and $(\Delta y')^2 = \frac{1}{64}$

and the resulting flow equations are

for liquid A: $u'_{A_1} + u'_{A_2} + u'_{A_3} + u'_{A_4} - 4u'_{A_o} + 0.12 = 0$ (18c)

at interface: $0.182u'_{B_1} + u'_{A_2} + 1.82u'_{A_3} + u'_{A_4} - 4u'_{A_o} + 0.23 = 0$ (20c)

and for liquid B: $u'_{B_1} + u'_{B_2} + u'_{B_3} + u'_{B_4} - 4u'_{B_o} + 1.25 = 0$ (19c)

These equations are solved as previously.

c. Results

Final point velocities are shown for grid sizes of $\frac{R}{2}$, $\frac{R}{4}$ and $\frac{R}{8}$ in figures 6,7 and 8 respectively, for the sample case of $y_i = \frac{R}{2}$ and $\mu' = 10$. Horizontal and vertical

velocity profiles for this case are shown in figures 9 and 10, respectively.

In figure 11, velocity profiles through the central vertical axis are compared for viscosity ratios of 10, 100 and 1000, with the interface again at $y_i = \frac{R}{2}$.

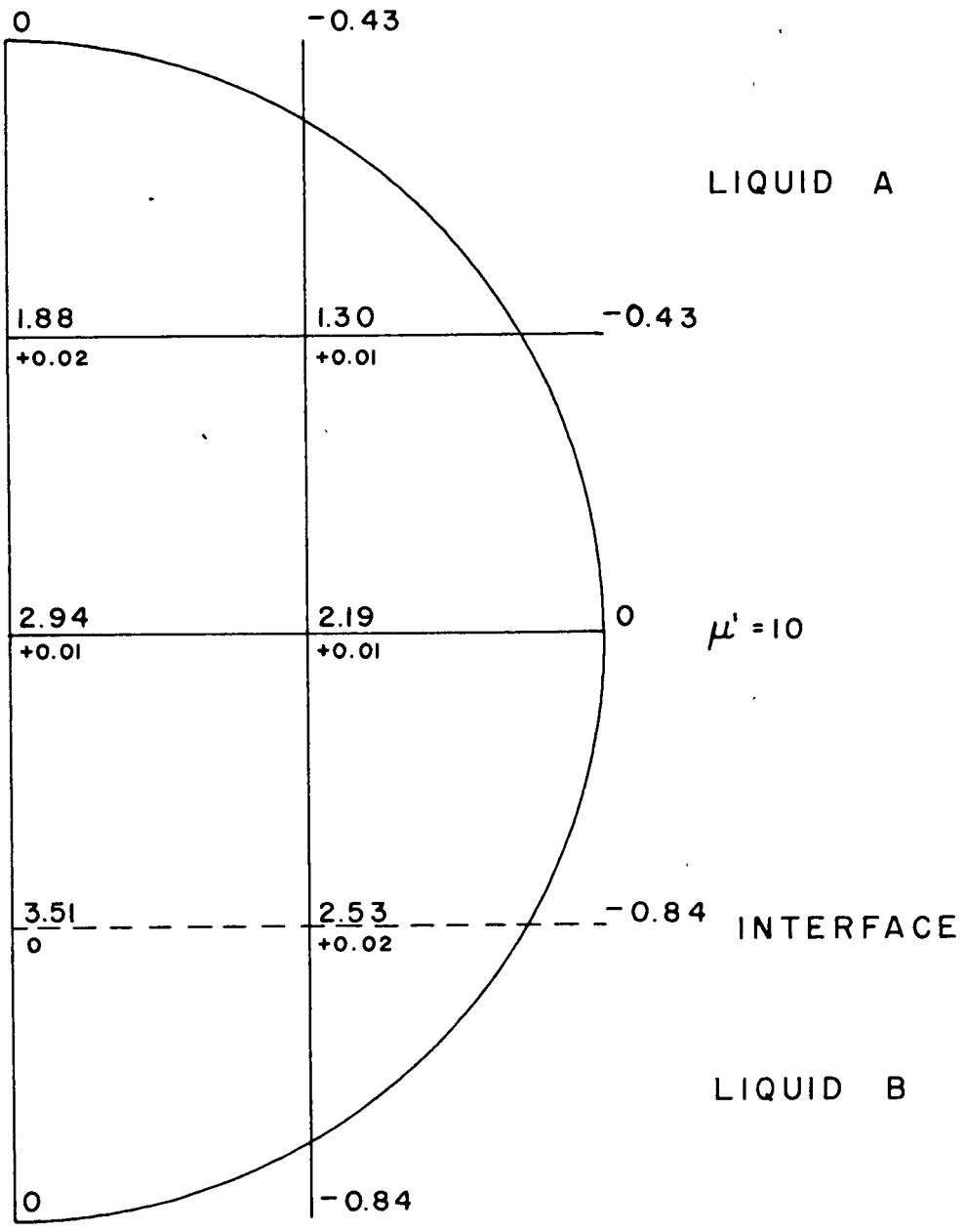

Figure 6. Sample of Final Point Velocities for Grid Size $\Delta y' = \frac{1}{2}$
(small numbers denote residuals)

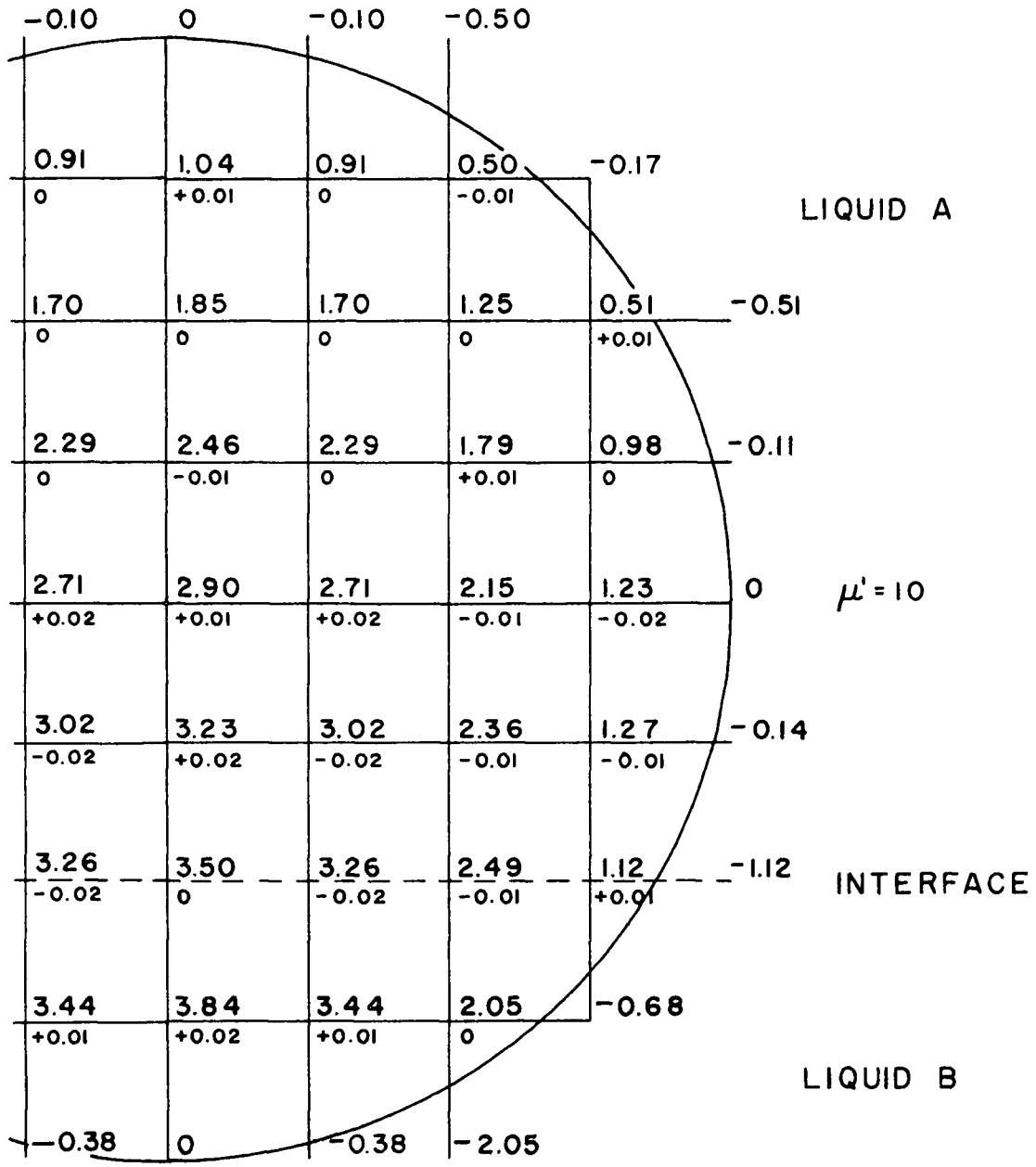

Figure 7. Sample of Final Point Velocities for Grid Size $\Delta y' = 1/4'$
(small numbers denote residuals)

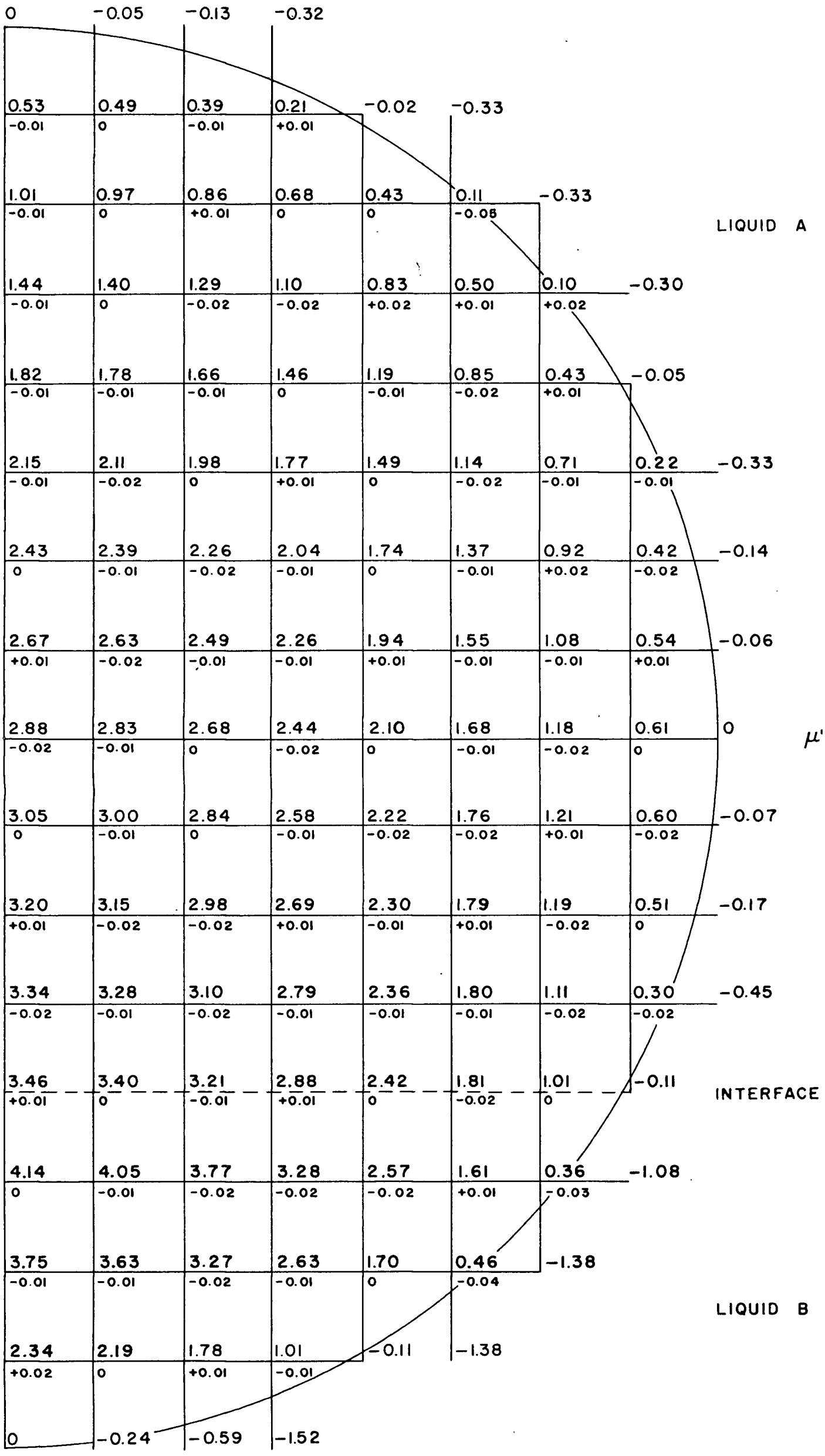

Figure 8. Sample of Final Point Velocities for Grid Size $\Delta y' = \frac{1}{8}$ (small numbers denote residuals)

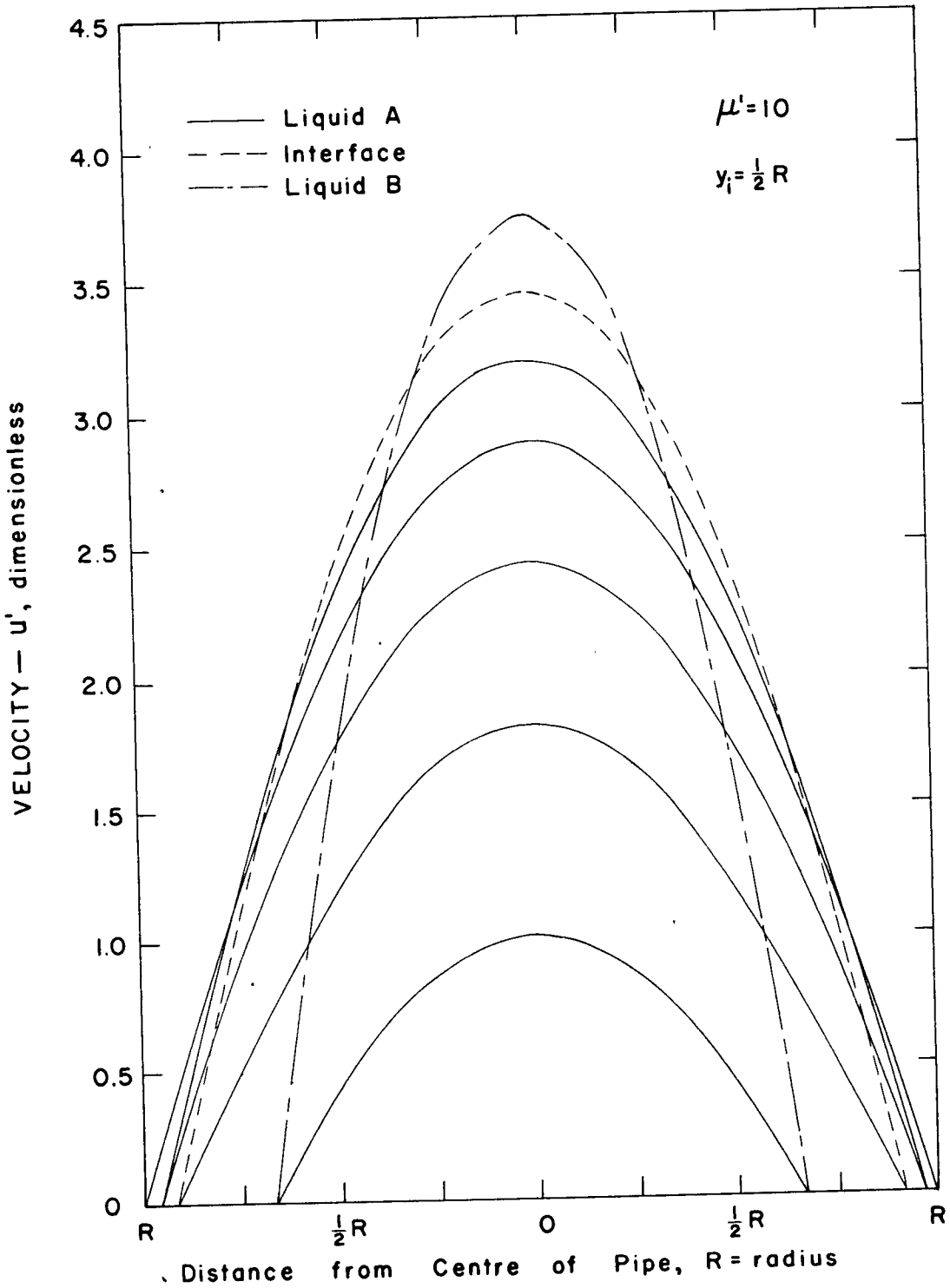

Figure 9. Horizontal Velocity Profiles for Interface at $y_i = \frac{R}{2}$, $\mu' = 10$

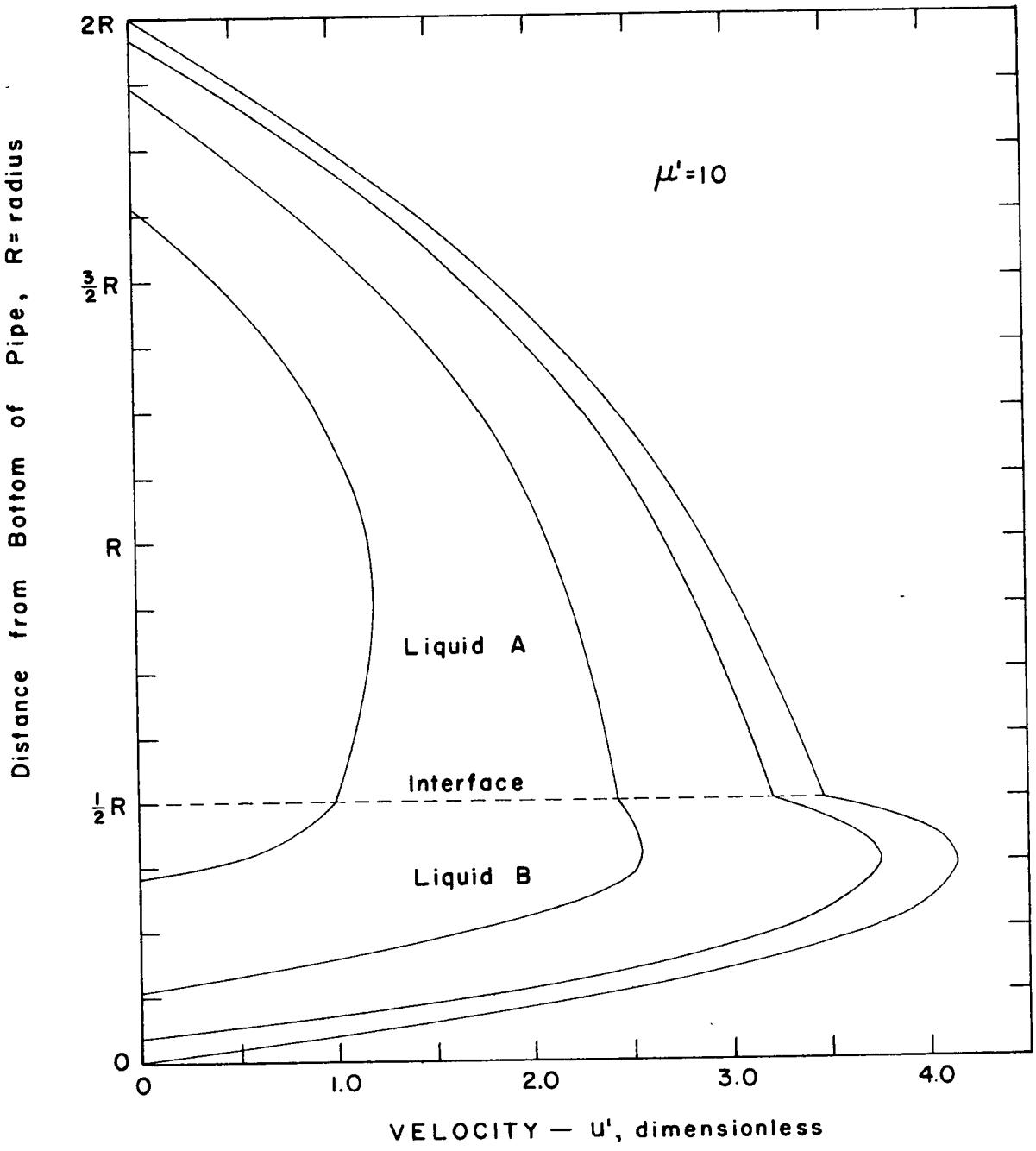

Figure 10. Vertical Velocity Profiles for Interface at $y_i = \frac{R}{2}$, $\mu' = 10$

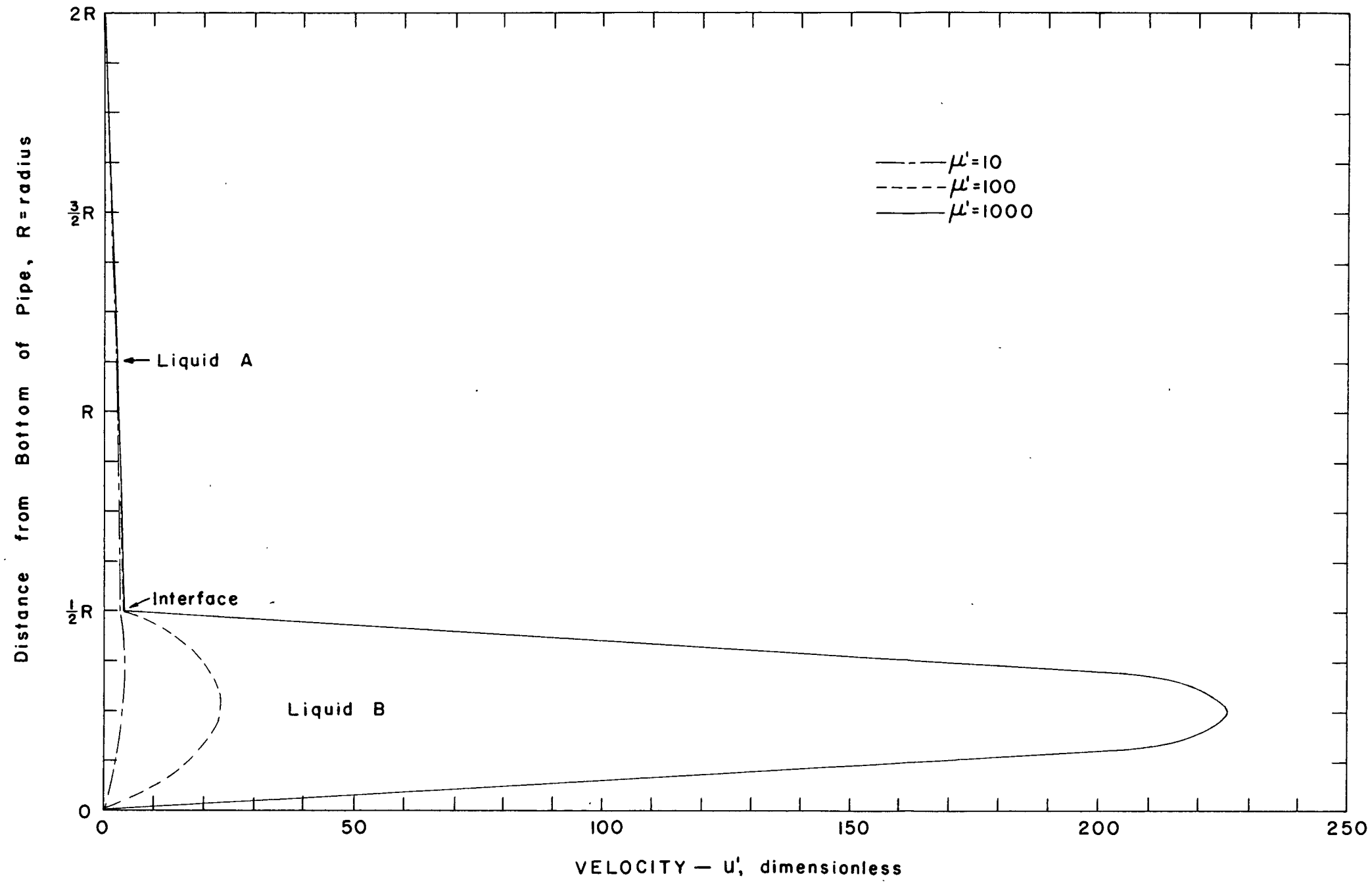

Figure 11. Central Vertical Velocity Profiles for μ'= 10, 100 and 1000, with Interface at $y_i = \frac{R}{2}$.

B. Volumetric Flow Rates

a. Theory

The volumetric flow rate is equal to the product of average velocity and cross-sectional area. Volumetric flow rates for the study are approximated by assuming that a nodal point in the grid is the average velocity for a square area of dimensions $\Delta y'$ by $\Delta z'$, with the nodal point at its centre. At the boundary, rectangular-like and triangular-like areas smaller than $(\Delta y')(\Delta z')$ are left over by this procedure. These areas are approximated by rectangles, and the average velocity computed as the arithmetic average of the velocities at the four corners of the rectangle. The velocities at the corners are found by interpolation between nodal velocities and boundary values. The product of the point velocities and the corresponding areas, including the boundary approximations, is expressed as $\Sigma u'_A(\Delta y')(\Delta z')$ for liquid A and as $\Sigma u'_B(\Delta y')(\Delta z')$ for liquid B. Transforming these expressions to absolute values the following relation holds:

$$\Sigma u'_A(\Delta y')(\Delta z') = \frac{\Sigma u_A(\Delta y)(\Delta z)}{U_A R^2} = \frac{Q_A}{Q_{Afull}/\pi} \qquad (23)$$

where Q_{Afull} is the volumetric flow rate for the pipe flowing full of liquid A, under the same pressure gradient as for the two-phase flow. The volumetric flow rate factor,

Q_A/Q_{Afull}, is an expression for comparing two-phase to one-phase flow at equal pressure gradients. Factors greater than unity constitute an advantage, because they signify that at the same pressure gradient, more liquid A can be transported by two-phase flow than by single-phase flow. Factors smaller than unity signify an opposite effect. The equation for evaluating the volumetric flow rate factor is

$$\frac{Q_A}{Q_{Afull}} = \frac{\Sigma u'_A(\Delta y')(\Delta z')}{\pi} \tag{23}$$

Previous authors (2) have compared pressure gradient reduction factors at constant volumetric flow rates. The following steps show the relationship between this factor and the volumetric flow rate factor of the present study.

Poiseuille's equation for one-phase laminar flow can be written as

$$\left(\frac{\partial P}{\partial x}\right)_{full} = c_1 \, Q_{A\ full} \tag{24}$$

Similarly, for two-phase flow, since equation (8) indicates direct proportionality between pressure gradient and velocity,

$$\left(-\frac{\partial P}{\partial x}\right) = c_2 \, Q_A \tag{25}$$

If $$-\left(\frac{\partial P}{\partial x}\right)_{full} = \left(-\frac{\partial P}{\partial x}\right),$$

then $$\frac{Q_A}{Q_{Afull}} = \frac{c_1}{c_2} \tag{26}$$

and if $$Q_{Afull} = Q_A,$$

then $$\frac{(-\frac{\partial P}{\partial x})_{full}}{(-\frac{\partial P}{\partial x})} = \frac{c_1}{c_2} \qquad (27)$$

Therefore $\frac{Q_A}{Q_{Afull}}$ at equal pressure gradients $= \frac{(-\frac{\partial P}{\partial x})_{full}}{(-\frac{\partial P}{\partial x})}$

at equal flow rates (28)

Thus the volumetric flow rate enhancement factor and the pressure gradient reduction factor are the same.

The maximum volumetric flow rate factor is calculated using the Douglass-Avakian method, as described in Appendix III, applied to the seven points, $\frac{R}{8}$ apart, between $y_i = 0$ and $y_i = \frac{3}{4}R$. A fourth degree polynomial is thus obtained, relating Q_A/Q_{Afull} to the interface position. This polynomial is differentiated and the result equated to zero, to give the value and location of the maximum volumetric flow rate factor.

b. Sample Calculations

Sample calculations for volumetric flow rates are based on the case of $\mu' = 10$ and an interface position of $y_i = \frac{R}{2}$. The final point velocities for this case are shown in figure 8.

For most interior points, except those near the boundaries, $(\Delta y')\ (\Delta z') = \frac{1}{64}$ and

$$\Sigma u'_A = 0.49 + 0.97 + 1.40 + 1.78 + 2.11 + 2.39 + 2.63$$
$$+ 2.83 + 3.00 + 3.15 + 3.28 + 0.39 + 0.86 + 1.29$$
$$+ 1.66 + 1.98 + 2.26 + 2.49 + 2.68 + 2.84 + 2.98$$
$$+ 3.10 + 0.68 + 1.10 + 1.46 + 1.77 + 2.04 + 2.26$$
$$+ 2.44 + 2.58 + 2.69 + 2.79 + 0.43 + 0.83 + 1.19$$
$$+ 1.49 + 1.74 + 1.94 + 2.10 + 2.22 + 2.30 + 2.36$$
$$+ 0.50 + 0.85 + 1.14 + 1.37 + 1.55 + 1.68 + 1.76$$
$$+ 1.79 + 1.80 + 0.43 + 0.71 + 0.92 + 1.08 + 1.18$$
$$+ 1.21 + 1.19 + 1.11 + 0.42 + 0.54 + 0.61 + 0.60$$
$$+ 0.51 = 105.92$$

At the vertical axis and interface $(\Delta y')(\Delta z') = \frac{1}{128}$ and

$$\Sigma \hat{u}'_A = 0.53 + 1.01 + 1.44 + 1.82 + 2.15 + 2.43 + 2.67$$
$$+ 2.88 + 3.05 + 3.20 + 3.34 + 3.40 + 3.21 + 2.88$$
$$+ 2.42 + 1.81 + 1.01 = 39.25$$

At the intersection of the vertical axis and the interface $(\Delta y')(\Delta z') = \frac{1}{256}$ and $u'_A = 3.46$.

For boundary areas approximated by $(\Delta y')(\Delta z') = \frac{1}{128}$

$$\Sigma u'_A = 0.12 + 0.27 + 0.22 + 0.23 + 0.23 + 0.22 + 0.27$$
$$+ 0.13 + 0.14 + 0.38 + 0.36 = 2.57$$

For boundary areas approximated by $(\Delta y')(\Delta z') = \frac{1}{256}$

$$\Sigma u'_A = 0.14 + 0.15 + 0.13 + 0.10 + 0.11 + 0.12 + 0.15$$
$$+ 0.12 = 1.02$$

For boundary areas approximated by $(\Delta y')(\Delta z') = \frac{1}{512}$

$$\Sigma u'_A = 0.08 + 0.06 + 0.08 + 0.06 + 0.06 + 0.09 = 0.43$$

Therefore $\Sigma u'_A(\Delta y')(\Delta z') = \frac{105.9}{64}$ or 1.655

$$+ \frac{(39.25+2.57)}{128} \text{ or } 0.3267$$

$$+ \frac{(3.46+1.02)}{256} \text{ or } 0.0175$$

$$+ \frac{0.43}{512} \text{ or } \frac{0.00084}{} = 2.00$$

This value is only for one half of the pipe; therefore for the whole pipe

$$\Sigma u'_A(\Delta y')(\Delta z') = 4.00$$

and $$\frac{Q_A}{Q_{Afull}} = \frac{4.00}{\pi} = 1.27$$

The volumetric flow rate summation for liquid B is performed in exactly the same manner. For the whole pipe, $\Sigma u'_B(\Delta y')(\Delta z') = 1.44$.

Sample calculations for locating the maximum volumetric flow rate factor are illustrated for a viscosity ratio of 10. The data for this case are presented in Table III. Letting $X = \frac{Q_A}{Q_{Afull}}$ and Y = interface position and following the Douglass - Avakian method, described in Appendix III, the calculation table below can be set up:

Y	X	Z =Y-0.375	k	kX	k^2X	k^3X	k^4X
0	1.00	-0.375	-3	-3.00	9.00	-27.00	81.00
0.125	1.12	-0.250	-2	-2.24	4.48	-8.96	17.92
0.250	1.20	-0.125	-1	-1.20	1.20	-1.20	1.20
0.370	1.27	0	0	0	0	0	0
0.500	1.27	0.125	1	1.27	1.27	1.27	1.27
0.625	1.18	0.250	2	2.36	4.72	9.44	18.88
0.750	1.06	0.375	3	3.18	9.54	28.62	85.86
				0.37	30.21	2.17	206.13

The constants in the polynomial $X = a+bZ+cZ^2+dZ^3+eZ^4$ are then calculated as

$$a = \frac{524(8.10) - 245(30.21) + 21(206.13)}{924} = 1.27$$

$$b = \frac{397(0.37)}{1512(0.125)} - \frac{7(2.17)}{216(0.125)} = 0.214$$

$$c = \frac{-840(8.10) + 679(30.21) - 67(206.13)}{3168\ (0.125)^2} = -2.06$$

$$d = \frac{-7(0.37) + 2.17}{216(0.125)^3} = -0.998$$

$$e = \frac{72(8.10) - 67(30.21) + 7(206.13)}{3168(0.125)^4} = 2.59$$

The fourth degree polynomial which fits the seven points best is then

$$X = 1.27 + 0.214\ Z - 2.06\ Z^2 - 0.998\ Z^3 + 2.59\ Z^4$$

and differentiating,

$$\frac{dX}{dZ} = 0 + 0.214 - 4.12\ Z - 2.99\ Z^2 + 10.4\ Z^3$$

At $Z = 0.050$, $\frac{dX}{dZ} = 0$

Therefore the maximum volumetric flow rate factor occurs at $Y = (0.050 + 0.375)R = 0.425R$ and the maximum value of

$\frac{Q_A}{Q_{A\,full}}$ is

$$X = 1.27 + 0.011 - 0.005 = 1.28$$

c. Calibration of Numerical Method

The numerical solution of stratified laminar flow of two liquids in a circular pipe was examined for accuracy by two methods. First, it was checked against the analytical results for single-liquid flow given by Poiseuille's equation. Secondly, similar numerical equations were derived for stratified flow of two liquids between parallel plates and solved by relaxation methods. These results were compared to the analytical results reported by Russell and Charles (2).

The dimensionless, numerical equation for single liquid flow is

$$u'_1 + u'_2 + u'_3 + u'_4 - 4u'_o + 8(\Delta y')^2 = 0 \qquad (18)$$

and for a grid size of $\Delta y = \frac{R}{8}$, equation (18) becomes

$$u'_1 + u'_2 + u'_3 + u'_4 - 4u'_o + 0.12 = 0$$

This equation was solved by relaxation methods to obtain dimensionless point velocities on the grid. In the first approximate solution, the residuals were unbalanced, that is, there was a predominance of either negative or positive residuals. Comparing this unbalanced numerical solution to the analytical solution of Poiseuille, the average per cent deviation of the velocities was 1.23%. The residuals

were then balanced so that the sum of all the residuals was approximately zero, and the average per cent deviation of the velocities in this case was 0.45%.

The volumetric flow rates were calculated for the two cases of unbalanced and balanced residuals. The analytical result is $\Sigma u'(\Delta y')(\Delta z') = \pi$, whereas for the unbalanced numerical solution, $\Sigma u'(\Delta y')(\Delta z') = 3.16$ and for the balanced numerical solution, $\Sigma u'(\Delta y')(\Delta z') = 3.14$. The deviation for the unbalanced solution was thus 0.64% and for the balanced case was undetectable in three significant figures. Throughout the investigation, the residuals were not completely balanced; the above results show that good agreement can nevertheless be expected.

For a larger grid size of $\Delta y = \frac{R}{4}$, $\Sigma u'(\Delta y')(\Delta z') = 3.26$, which is a deviation of 3.8% from the analytical result. Therefore a grid size of $\Delta y = \frac{R}{8}$ was chosen, because of the better agreement with the analytical result.

When the interface was a distance $\frac{R}{8}$ above the bottom of the pipe, there were no grid points in the region of flow of liquid B with a grid size of $\Delta y = \frac{R}{8}$. Therefore a grid size of $\Delta y = \frac{R}{16}$ was used. Errors in the calculation of $\Sigma u'_B(\Delta y')(\Delta z')$ using the larger grid, especially at high viscosity ratios, were eliminated by using the smaller grid for which point velocities could be obtained in the main body of liquid B.

A solution for two-phase flow with the interface a distance $\frac{R}{2}$ above the bottom of the pipe and a grid size of $\Delta y = \frac{R}{8}$ was calculated using three-figure accuracy, then recalculated using two-figure accuracy. As the difference in the volumetric flow rate factors was 3.6%, all calculations were subsequently performed with three-figure accuracy.

The numerical solution was also checked against an analogous case of stratified laminar flow of two liquids between infinite parallel plates. Numerical equations for this model were derived in a manner similar to those derived in the present investigation, and are

$$\text{for liquid A:} \quad u'_{A_1} + u'_{A_3} - 2u'_o + 3(\Delta y')^2 = 0 \tag{29}$$

$$\text{at interface:} \quad \frac{2}{\mu'+1} u'_{B_1} + \frac{2\mu'}{\mu'+1} u'_{A_3} - 2u'_{A_o} + \frac{6\mu'}{\mu'+1}(\Delta y')^2 = 0 \tag{30}$$

$$\text{and for liquid B:} \quad u'_{B_1} + u'_{B_3} - 2u'_{B_o} + 3\mu'(\Delta y')^2 = 0 \tag{31}$$

These dimensionless equations were solved by relaxation methods for the case of $\mu' = 1000$ and the interface at $y_i = s$, where the plates are a distance 2s apart, using a grid size of $\Delta y = \frac{s}{8}$. The point velocities were solved analytically using the expressions given by Russell and Charles (2). The two results are shown in figure 12, where it is seen that all corresponding point velocities match up exactly for three-figure accuracy.

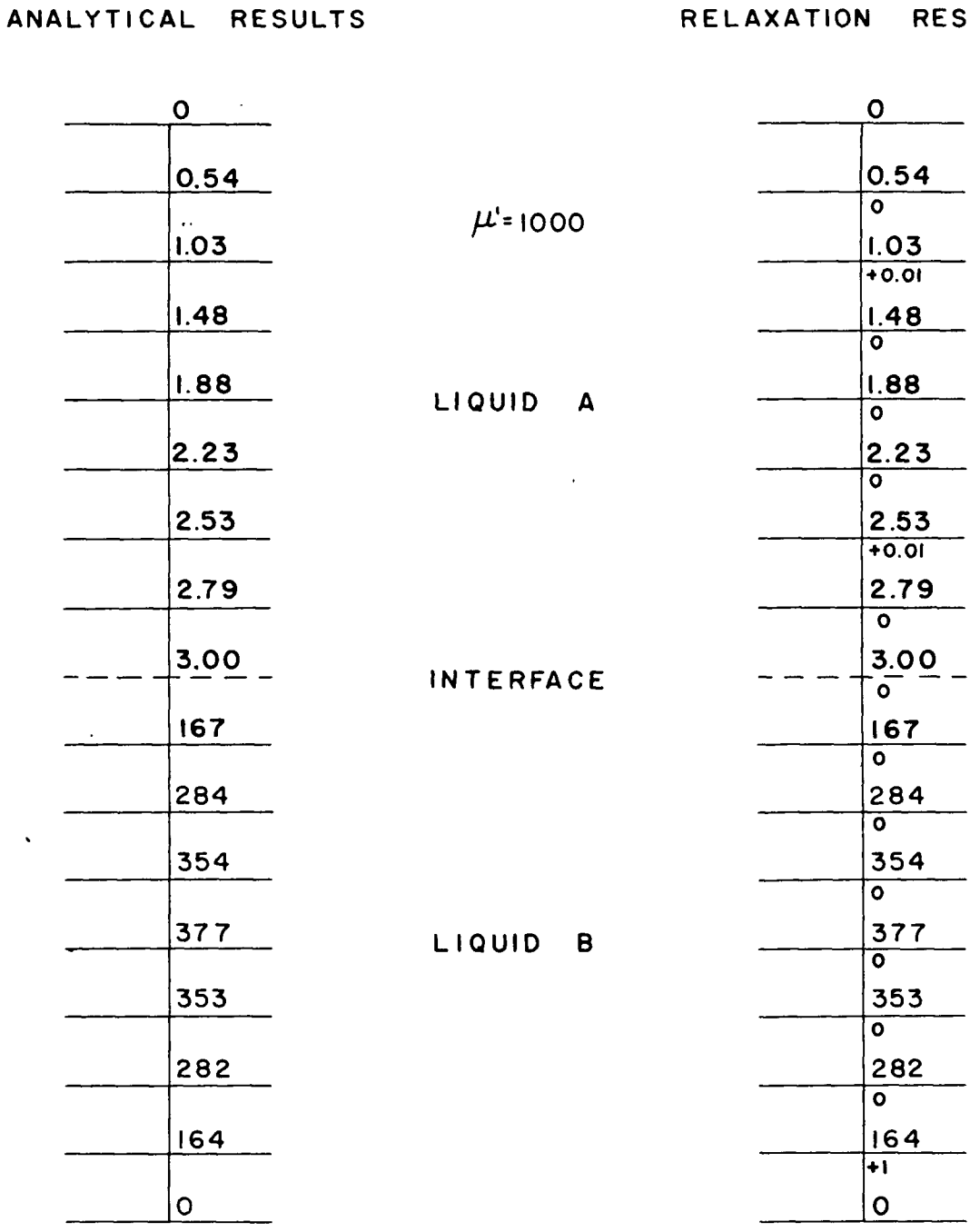

Figure 12. Comparison of Analytical and Relaxation Results for Parallel Plate Flow

These two checks show that the numerical solution employed in this study agrees extremely well with those analytical solutions available, and can therefore be considered very reliable for the three significant figures reported.

d. Results

Calculated values of the numerical flow rate factors for different interface positions are presented in Tables II, III, IV and V for viscosity ratios of 1,10,100 and 1000 respectively.

In figure 13, the volumetric flow rate factor is plotted against the interface position for the four viscosity ratios investigated. Flow area fractions were calculated from the interface positions as described in Appendix II, and figure 14 is a plot of volumetric flow rate factor versus flow area fraction of liquid B for all four viscosity ratios. The maximum volumetric flow rate factors, recorded in Table VI are plotted in figure 15 against the viscosity ratios.

Table II

Volumetric Flow Rates, $\mu' = 1.0$

y_i	$\Sigma u'_A(\Delta y')(\Delta z')$	$\Sigma u'_B(\Delta y')(\Delta z')$	$\frac{Q_A}{Q_{Afull}}$
0	3.16	0	1.00
R/8	3.14	0.02	0.994
R/4	3.07	0.09	0.972
3R/8	2.94	0.22	0.930
R/2	2.75	0.41	0.870
5R/8	2.51	0.65	0.794
3R/4	2.22	0.94	0.703
7R/8	1.91	1.25	0.604
R	1.58	1.58	0.500
9R/8	1.25	1.91	0.396
5R/4	0.94	2.22	0.297
11R/8	0.65	2.51	0.206
3R/2	0.41	2.75	0.130
13R/8	0.22	2.94	0.070
7R/4	0.09	3.07	0.026
15R/8	0.02	3.14	0.006
2R	0	3.16	0

Table III

Volumetric Flow Rates, $\mu' = 10$

y_i	$\Sigma u'_A(\Delta y')(\Delta z')$	$\Sigma u'_B(\Delta y')(\Delta z')$	$\frac{Q_A}{Q_{Afull}}$
0	3.14	0	1.00
R/8	3.53	0.0614	1.12
R/4	3.76	0.282	1.20
3R/8	3.99	0.724	1.27
R/2	4.00	1.44	1.27
5R/8	3.72	2.45	1.18
3R/4	3.33	3.80	1.06
R	2.43	7.78	0.774
3R/2	0.590	20.1	0.188
2R	0		0

Table IV

Volumetric Flow Rates, $\mu' = 100$

y_i	$\Sigma u'_A(\Delta y')(\Delta z')$	$\Sigma u'_B(\Delta y')(\Delta z')$	$\frac{Q_A}{Q_{Afull}}$
0	3.14	0	1.00
R/8	3.85	0.127	1.23
R/4	4.17	0.801	1.33
3R/8	4.34	2.92	1.38
R/2	4.31	7.24	1.37
5R/8	3.95	14.6	1.26
3R/4	3.50	25.6	1.11
R	2.55	61.2	0.812
3R/2	0.615	188	0.196
2R	0		0

Table V

Volumetric Flow Rates, $\mu' = 1000$

y_i	$\Sigma u'_A(\Delta y')(\Delta z')$	$\Sigma u'_B(\Delta y')(\Delta z')$	$\frac{Q_A}{Q_{Afull}}$
0	3.14	0	1.00
R/8	3.93	0.559	1.25
R/4	4.27	5.47	1.36
3R/8	4.42	24.0	1.41
R/2	4.39	64.1	1.40
5R/8	4.02	135	1.28
3R/4	3.56	242	1.13
R	2.60	596	0.828
3R/2	0.619	1860	0.196
2R	0		0

Table VI

Maximum Volumetric Flow Rate Factors

Viscosity Ratio, μ'	1.0	10	100	1,000
Maximum $\frac{Q_A}{Q_{A\,full}}$	1.00	1.28	1.38	1.41
Interface Position, y_i	0	0.425R	0.390R	0.385R

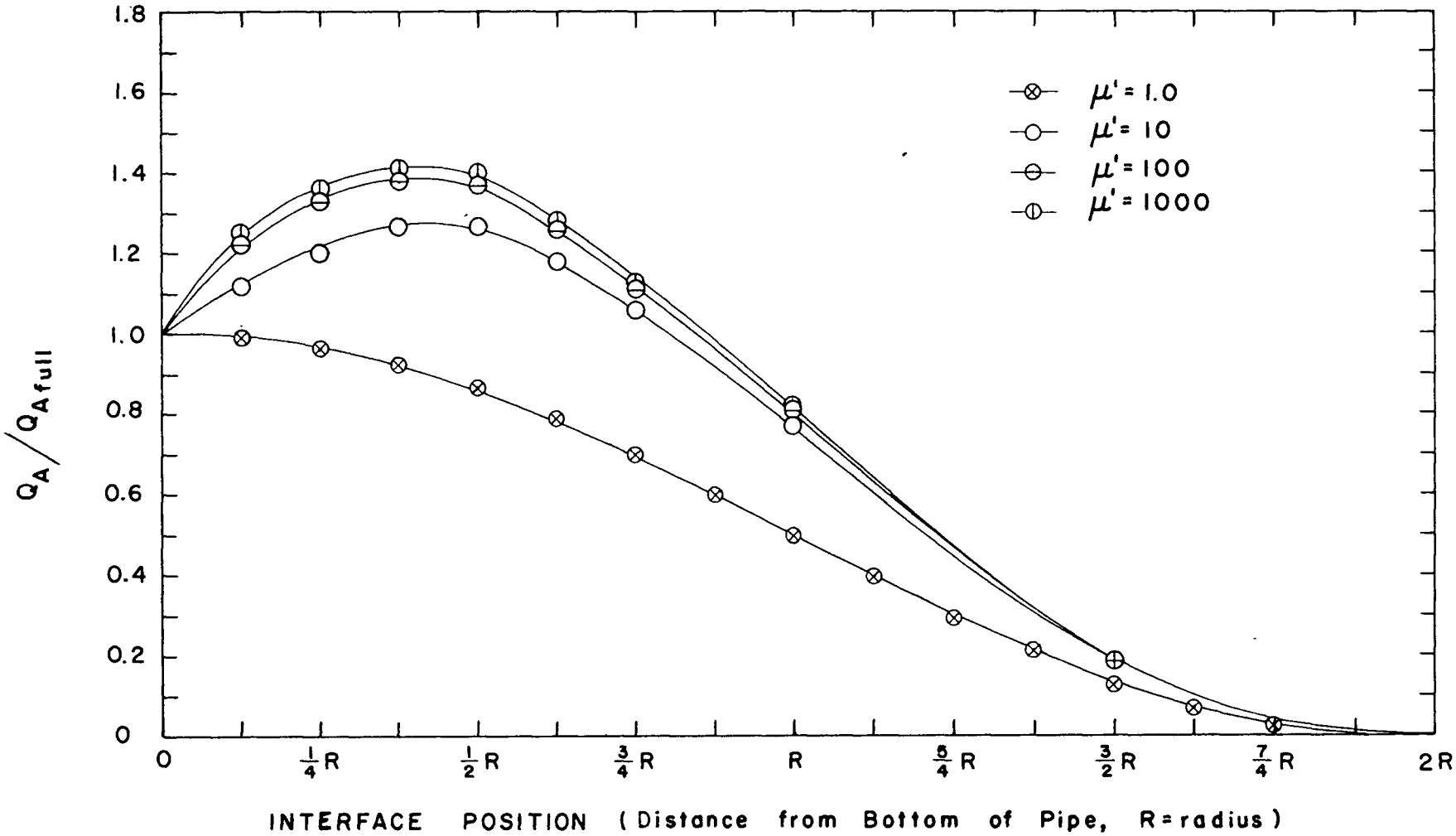

Figure 13. Variation of Volumetric Flow Rate Factor with Interface Position

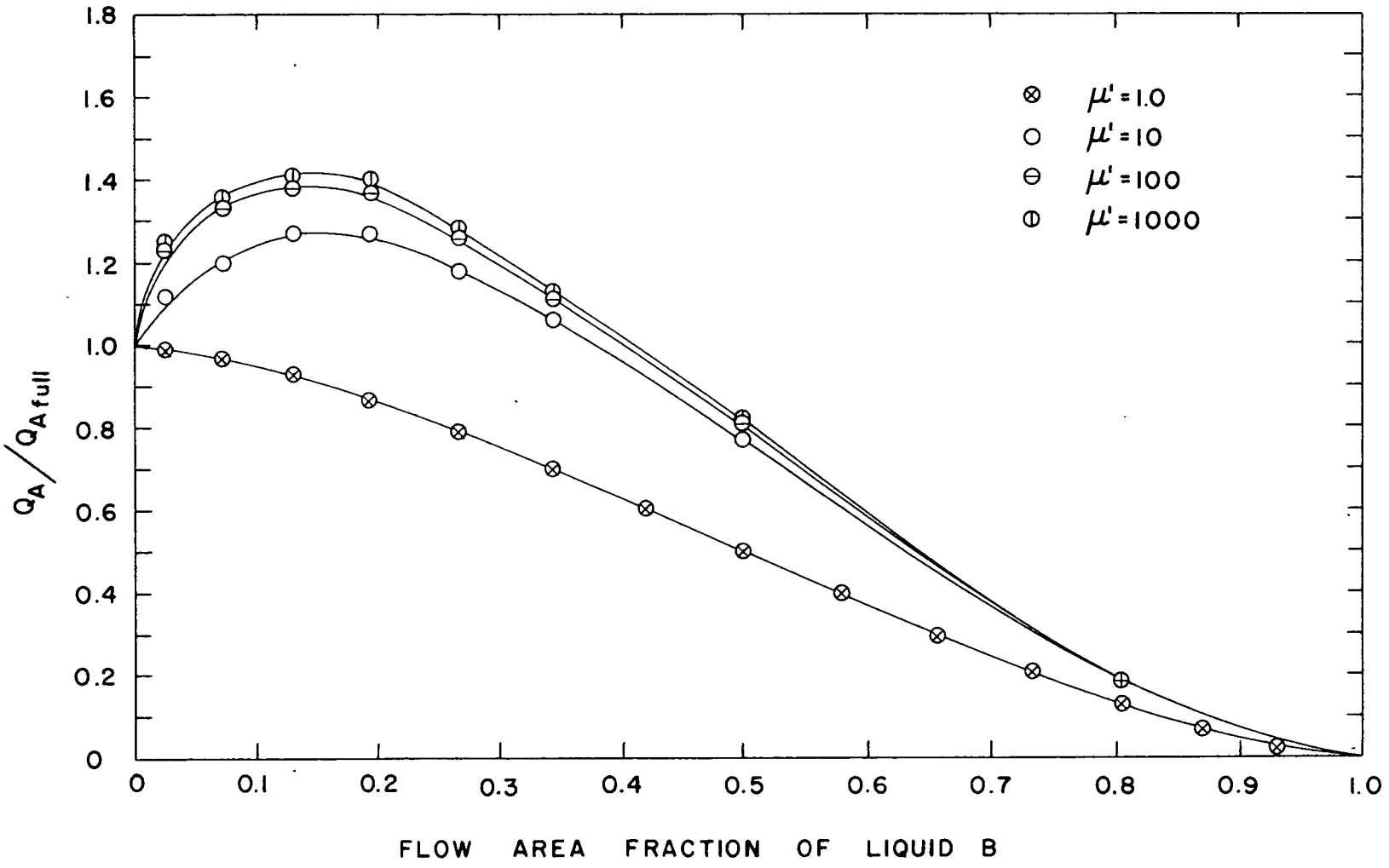

Figure 14. Variation of Volumetric Flow Rate Factor with Flow Area Fraction

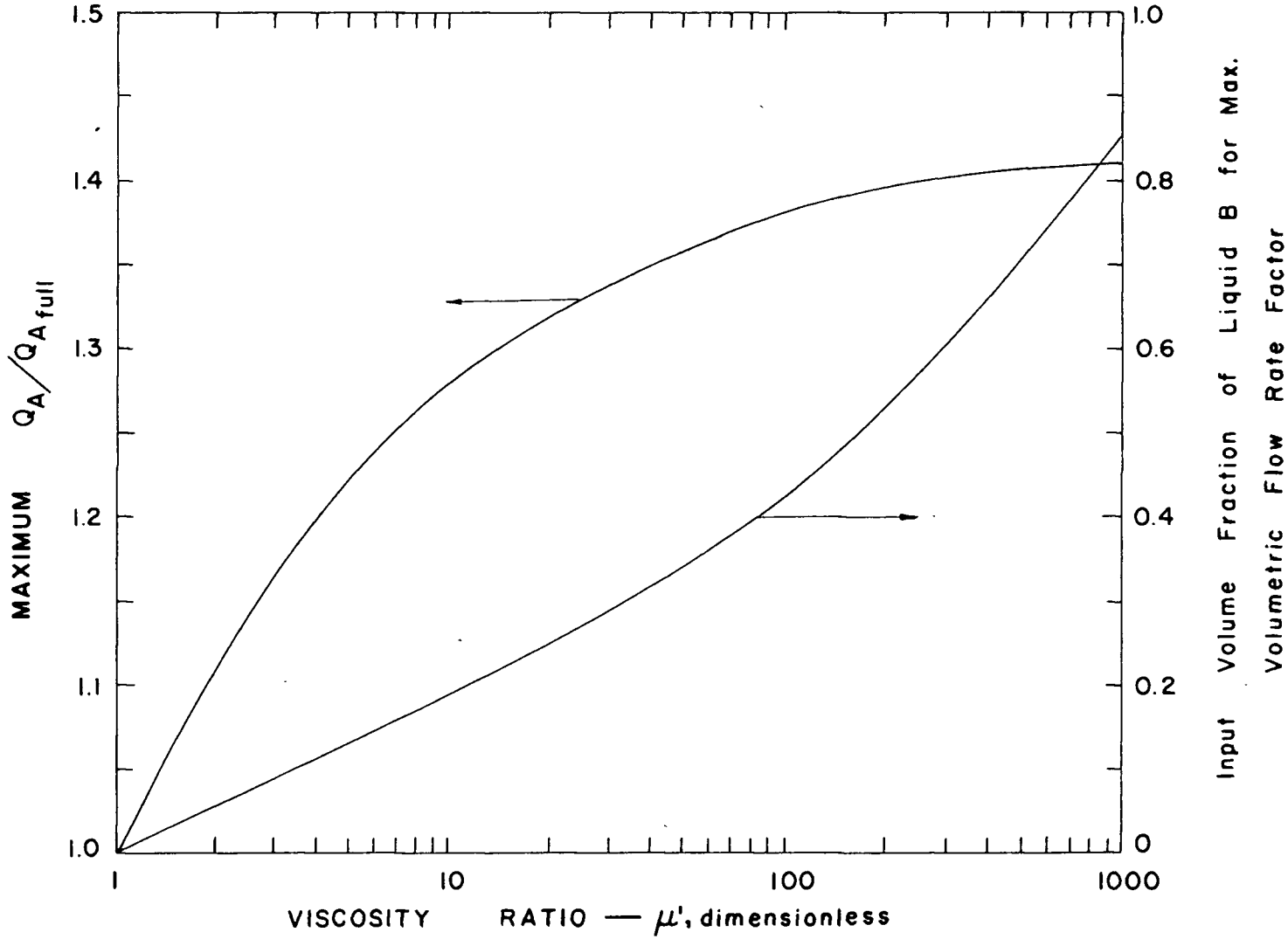

Figure 15. Maximum Volumetric Flow Rate Factors and Corresponding Input Volume Fractions for Various Viscosity Ratios

C. Power Requirements

a. Theory

The power requirement per unit length of pipe is the product of the pressure drop per unit length and the total volumetric flow rate of both liquids. In the case of two-phase flow, it is expressed as

$$\frac{\text{Power}}{x} = W = \left(-\frac{\partial P}{\partial x}\right)(Q_A + Q_B) \tag{32}$$

and for the pipe flowing full of liquid A, as

$$W_{full} = \left(-\frac{\partial P}{\partial x}\right)_{full}(Q_{Afull}) \tag{33}$$

If $Q_A = Q_{Afull}$

$$\frac{W_{full}}{W} = \left[\frac{\left(-\frac{\partial P}{\partial x}\right)_{full}}{\left(-\frac{\partial P}{\partial x}\right)} \text{ for constant } Q_A\right]\left[\frac{Q_A}{Q_A+Q_B}\right] \tag{34}$$

and from equation (28),

$$\frac{W_{full}}{W} = \left[\frac{Q_A}{Q_{Afull}} \text{ for constant}\left(-\frac{\partial P}{\partial x}\right)\right]\left[\frac{1}{1+\frac{Q_B}{Q_A}}\right] \tag{35}$$

i.e.

$$\frac{W_{full}}{W} = \frac{Q_A}{Q_{Afull}} \quad \frac{1}{1 + \frac{\Sigma u'_A(\Delta y')(\Delta z')}{\Sigma u'_B(\Delta y')(\Delta z')}} \tag{36}$$

and therefore the power reduction factor, $\frac{W_{full}}{W}$, is easily calculated from the data of the previous section.

To obtain the maximum power reduction factor and thus the minimum power requirement for two-phase flow, the Douglass - Avakian method was applied over seven equidistant points, at increments of $\frac{R}{16}$. The smaller increments were chosen because the maximum power reduction factors occur at interface positions closer to the bottom of the pipe, and the plot of power reduction factor versus interface position has a greater curvature, than in the case of volumetric flow rate factors.

Since the previous calculations were for increments of $\frac{R}{8}$, the intermediate values for increments of $\frac{R}{16}$ were obtained by interpolation of the previous data. From the polynomial relating $\frac{Q_A}{Q_{Afull}}$ and interface position, the volumetric flow rate factors for the intermediate points were determined and by equation (23), $\Sigma u'_A(\Delta y')(\Delta z')$ was calculated. Intermediate values of $\Sigma u'_B(\Delta y')(\Delta z')$ were interpolated from a polynomial of the form, $X = a+bY+cY^2+dY^3$, where $X = \Sigma u'_B(\Delta y')(\Delta z')$ and Y was the interface position. The constants of the polynomial were evaluated from four pairs of values calculated previously for increments of $\frac{R}{8}$. The Douglass - Avakian method was not used with the larger increments because the values of X for seven equidistant values of Y varied greatly in magnitude, and the resulting relationship, though it was the best fourth degree polynomial for the seven points, was not accurate enough in the region of the maximum power reduction factor. The Douglass - Avakian method, followed by differentiation, was, however,

applied to the smaller increments to obtain the value and location of the maximum power reduction factors.

b. Sample Calculations

Sample calculations for power reduction factor are based on the case of $\mu' = 10$ and the interface at $y_i = \frac{R}{2}$.

$$\frac{Q_A}{Q_{Afull}} = 1.27$$

$$\Sigma u'_A(\Delta y')(\Delta z') = 4.00$$

$$\Sigma u'_B(\Delta y')(\Delta z') = 1.44$$

and $$\frac{W_{full}}{W} = (1.27) \quad \frac{1}{1 + \frac{1.44}{4.00}} = 0.933$$

A sample determination of the maximum power reduction factor is based on values for a viscosity ratio of 10. Calculations are shown for obtaining values at the intermediate point of $y = \frac{3R}{16} = 0.1875R$. Considering first the liquid A, and letting $X = \frac{Q_A}{Q_{Afull}}$ and Y = interface position such that $Y = \frac{3R}{8}$ corresponds to Z = 0, the Douglass - Avakian method gave the following polynomial

$$X = 1.27 + 0.214Z - 2.06Z^2 - 0.998Z^3 + 2.59Z^4$$

At an interface position of $Y = \frac{3R}{16}$ or Z = -0.1875

$$X = 1.27+0.214(-0.1875)-2.06(-0.1875)^2-0.998(-0.1875)^3 + 2.59(-0.1875)^4,$$

that is $\frac{Q_A}{Q_{Afull}} = 1.17$

and therefore $\Sigma u'_A(\Delta y')(\Delta z') = \pi\ (1.17) = 3.68$

For liquid B, the following results were obtained:

Y	$\Sigma u'_B(\Delta y')(\Delta z')$
0	0
R/8	0.0614
R/4	0.282
3R/8	0.724

If $X = \Sigma u'_B(\Delta y')(\Delta z')$ and Y = interface position, their relationship can be given by the polynomial, $X = a+bY+cY^2+dY^3$. Substitution of the above values and solution for the constants resulted in the polynomial

$$X = 0.012Y + 3.19Y^2 + 5.10Y^3.$$

At $Y = \frac{3}{16}$,

$$X = 0.012(0.1875)+3.19(0.1875)^2+5.10(0.1875)^3=0.148$$

and therefore $\frac{W_{full}}{W} = (1.17)\ \frac{1}{1 + \frac{0.148}{3.68}} = 1.12$

Other intermediate values were obtained for interface positions of $\frac{R}{16}$ and $\frac{5R}{16}$. The seven equidistant points between Y = 0 and $Y = \frac{3R}{8}$ were then used to obtain the value and location of the maximum power reduction factor by the Douglass - Avakian method, followed by differentiation, in a manner identical to that used for determining the maximum

volumetric flow rate factor.

c. Results

Results for power reduction factors are presented in Table VII for viscosity ratios of 10, 100 and 1000.

In figure 16, the power reduction factors are plotted against the interface position for the three viscosity ratios. These factors are then replotted against the fractional flow area in figure 17. A graph of the maximum power requirement factor against the viscosity ratio is shown in figure 18, based on results recorded in table VIII.

Table VII

Power Reduction Factors

y_i	$\frac{W_{full}}{W}$		
	$\mu' = 10$	$\mu' = 100$	$\mu' = 1000$
0	1.00	1.00	1.00
R/16*	1.05	1.10	1.05
R/8	1.10	1.19	1.10
3R/16	1.12	1.20	0.897
R/4*	1.11	1.12	0.597
5R/16*	1.12	0.995	0.366
3R/8	1.08	0.828	0.220
R/2	0.933	0.511	0.0897
5R/8	0,710	0.268	0.0370
3R/4	0.495	0.133	0.0164
R	0.184	0.0325	0.00435
3R/2	0.00536	0.000639	0.0000656
2R	0	0	0

(* - interpolated position)

Table VIII

Maximum Power Reduction Factors

Viscosity Ratio, μ'	10	100	1000
Maximum $\frac{W_{full}}{W}$	1.12	1.22	1.09 (1.1)
Interface Position, y_i	0.267R (0.27R)	0.170R (0.17R)	0.09R (0.1R)

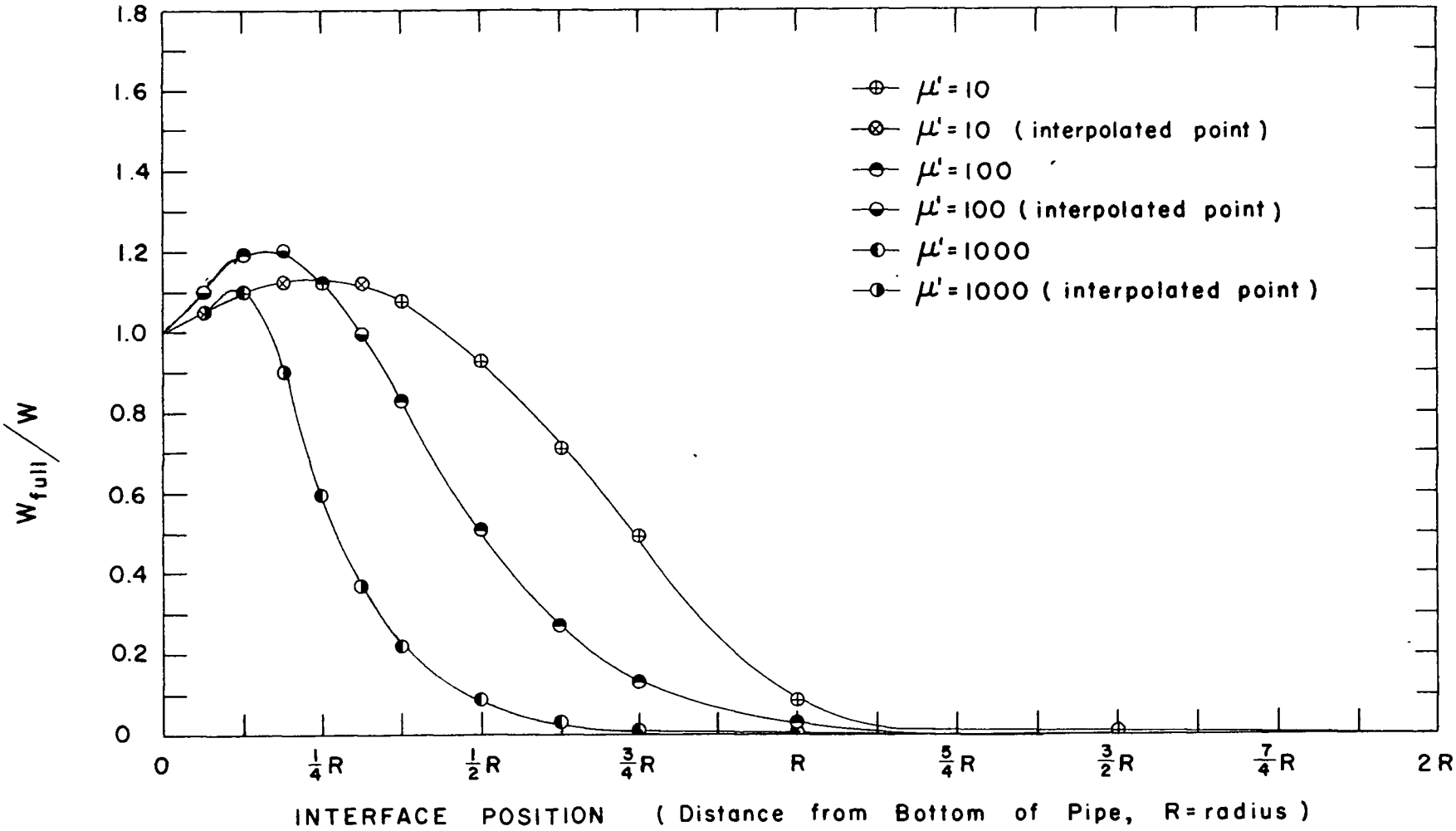

Figure 16. Variation of Power Reduction Factor with Interface Position

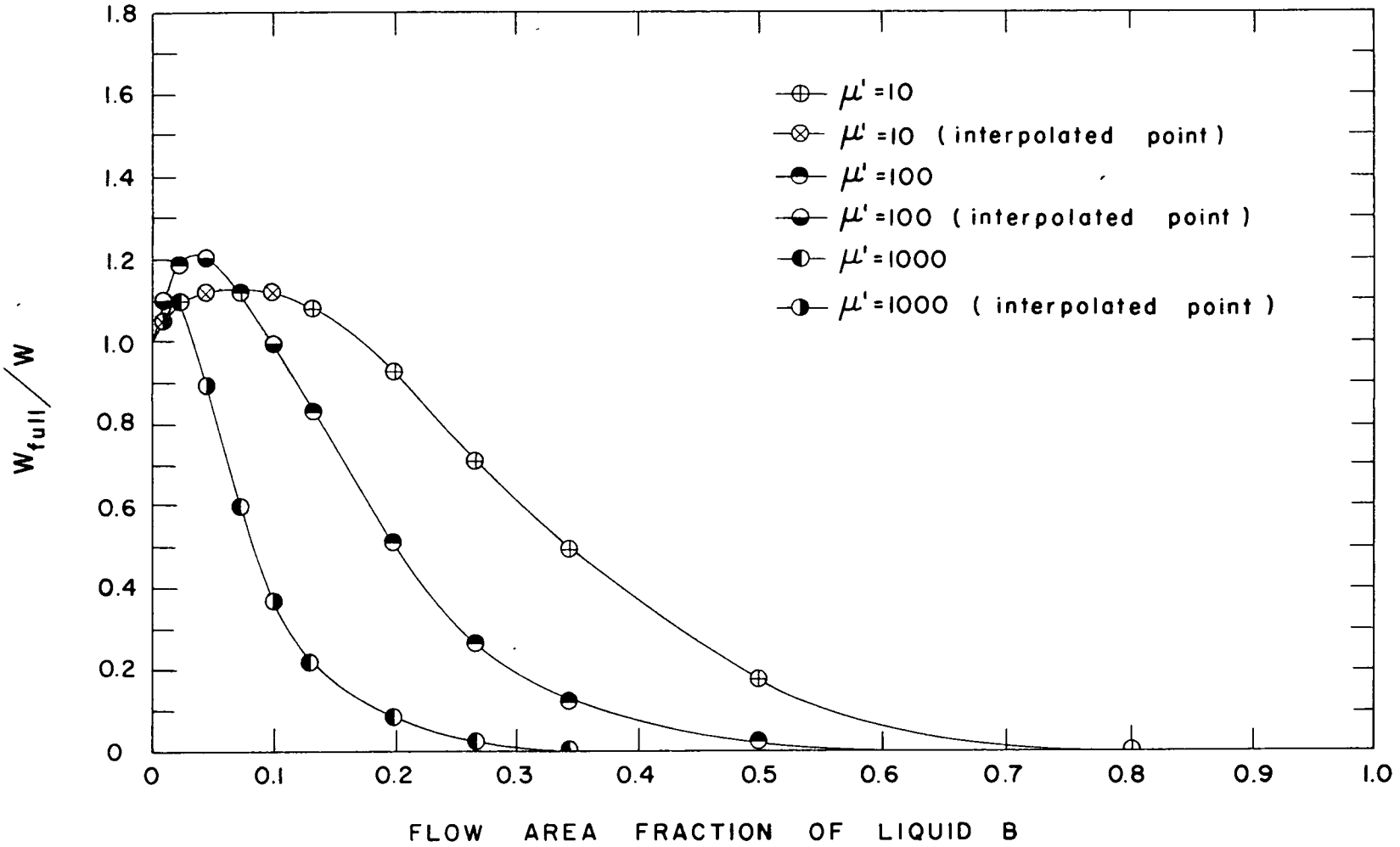

Figure 17. Variation of Power Reduction Factor with Flow Area Fraction

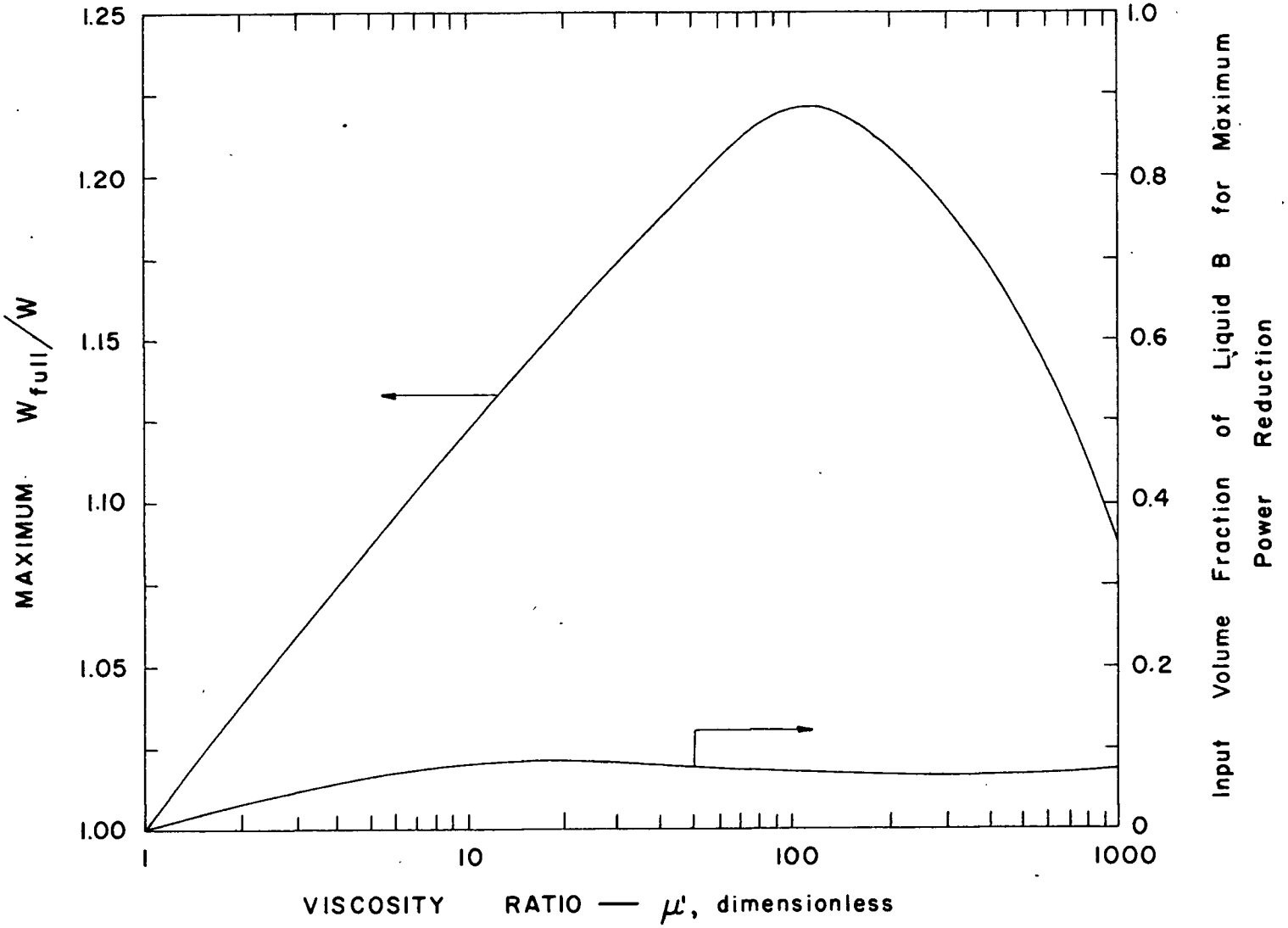

Figure 18. Maximum Power Reduction Factors and Corresponding Input Volume Fractions for Various Viscosity Ratios

D. Hold-up Ratios

a. Theory

The hold-up ratio is defined as the input volume ratio divided by the in situ volume ratio. The input volume ratio is the volumetric flow rate of liquid A divided by the volumetric flow rate of liquid B, and in this study it is evaluated as

$$\text{input volume ratio} = \frac{\Sigma u'_A(\Delta y')(\Delta z')}{\Sigma u'_B(\Delta y')(\Delta z')} \qquad (37)$$

The in situ volume ratio is the ratio of the volumes of A and B inside the pipe, and for steady stratified flow of incompressible liquids may be expressed as

$$\text{in situ volume ratio} = \frac{\text{flow area of liquid A}}{\text{flow area of liquid B}} \qquad (38)$$

Therefore

$$\text{hold-up ratio} = \frac{\Sigma u'_A(\Delta y')(\Delta z')}{\Sigma u'_B(\Delta y')(\Delta z')} \Big/ \frac{\text{flow area of liquid A}}{\text{flow area of liquid B}} \qquad (39)$$

A plot of hold-up ratio versus input volume ratio can be made for different viscosity ratios, to illustrate the point that the hold-up ratio is independent of liquid velocities for laminar flow, as realized by Russell, Hodgson and Govier (6).

b. Sample Calculations

Calculations are based on the case of $\mu' = 10$ and $y_i = \frac{R}{2}$.

As shown previously, $\Sigma u'_A(\Delta y')(\Delta z') = 4.00$

and $\Sigma u'_B(\Delta y')(\Delta z') = 1.44$

Therefore input volume ratio $= \frac{4.00}{1.44} = 2.78$

Flow area of liquid A $= 2.53\ R^2$

Flow area of liquid B $= 0.614\ R^2$

Hence in situ volume ratio $= \frac{2.53}{0.614} = 4.12$

and therefore

hold-up ratio $= \frac{2.78}{4.12} = 0.675$

c. Results

Table IX contains the results for input volume ratio, in situ volume ratio and hold-up ratio for viscosity ratios of 1, 10, 100 and 1000. In figure 19 hold-up ratio is plotted against input volume ratio for four viscosity ratios.

Graphs of volumetric flow rate factor and power reduction factor versus input volume fraction could now be made and are shown in figure 20 and 21, respectively. Also, input volume fractions for the maximum volumetric flow rate factors and for the maximum power reduction factors could be calculated, and these values are plotted in figures 15 and 18, respectively, for various viscosity ratios.

Table IX

Calculated Hold-up Data

y_i	Input Volume Ratio μ'				In Situ Volume Ratio	Hold-up Ratio μ'			
	1.0	10	100	1000		1.0	10	100	1000
0	∞	∞	∞	∞		∞	∞	∞	∞
R/8	157	57.5	30.3	7.03	38.3	4.10	1.50	0.791	0.184
R/4	34.1	13.3	5.21	0.781	12.8	2.66	1.04	0.407	0.0610
3R/8	13.4	5.51	1.49	0.184	6.69	2.00	0.834	0.223	0.0275
R/2	6.71	2.78	0.595	0.0685	4.12	1.63	0.675	0.144	0.0166
5R/8	3.86	1.52	0.271	0.0298	2.74	1.41	0.555	0.0989	0.0109
3R/4	2.36	0.876	0.137	0.0147	1.91	1.24	0.459	0.0717	0.00770
7R/8	1.53				1.38	1.11			
R	1.00	0.312	0.0417	0.00436	1.00	1.00	0.312	0.0417	0.00436
9R/8	0.654				0.725	0.902			
5R/4	0.423				0.524	0.807			
11R/8	0.259				0.365	0.710			
3R/2	0.149	0.0294	0.00327	0.000333	0.243	0.613	0.121	0.0135	0.00137
13R/8	0.0748				0.149	0.502			
7R/4	0.0293				0.0781	0.375			
15R/8	0.00637				0.0261	0.244			
2R	0	0	0	0	0	0	0	0	0

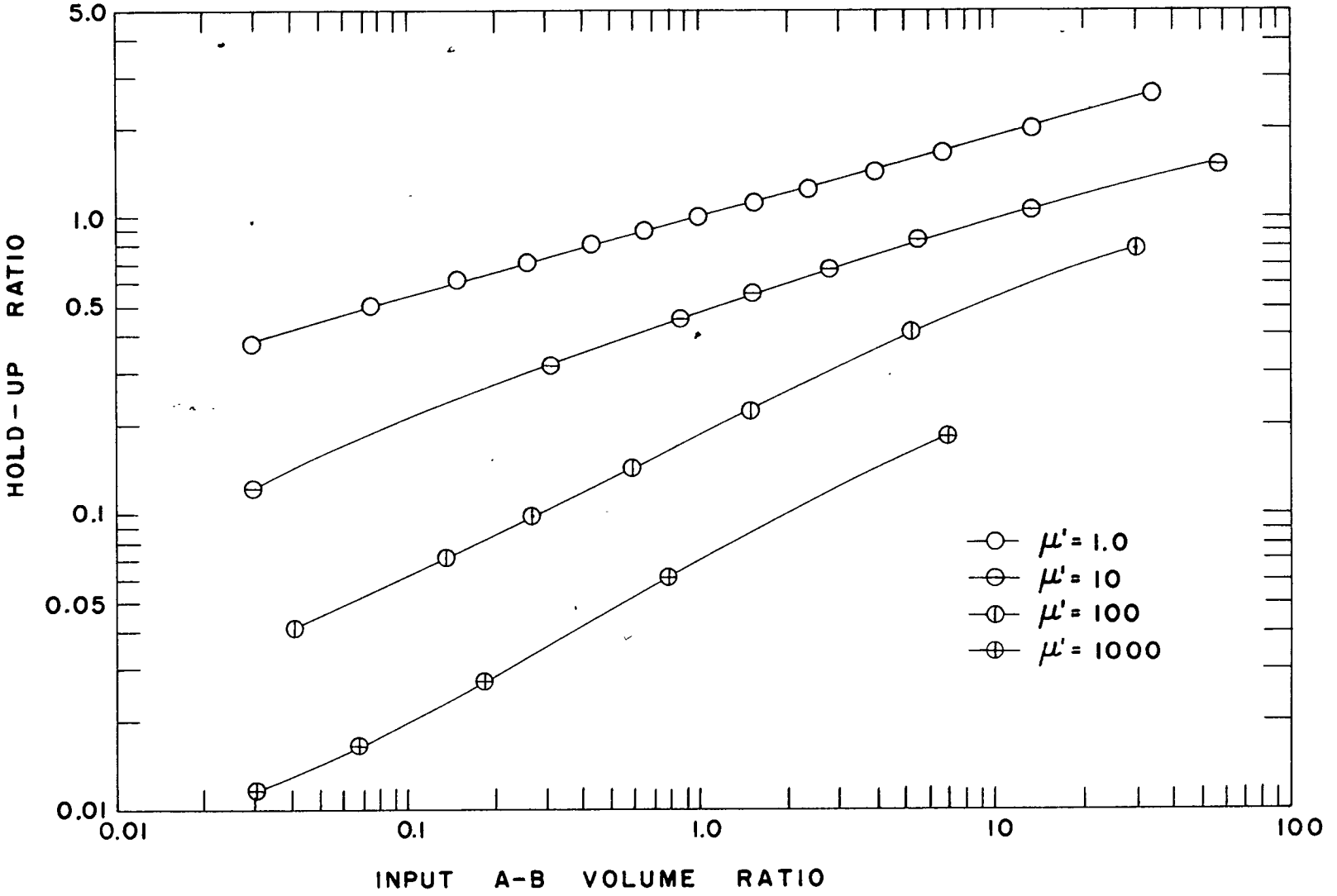

Figure 19. Hold-up Ratios

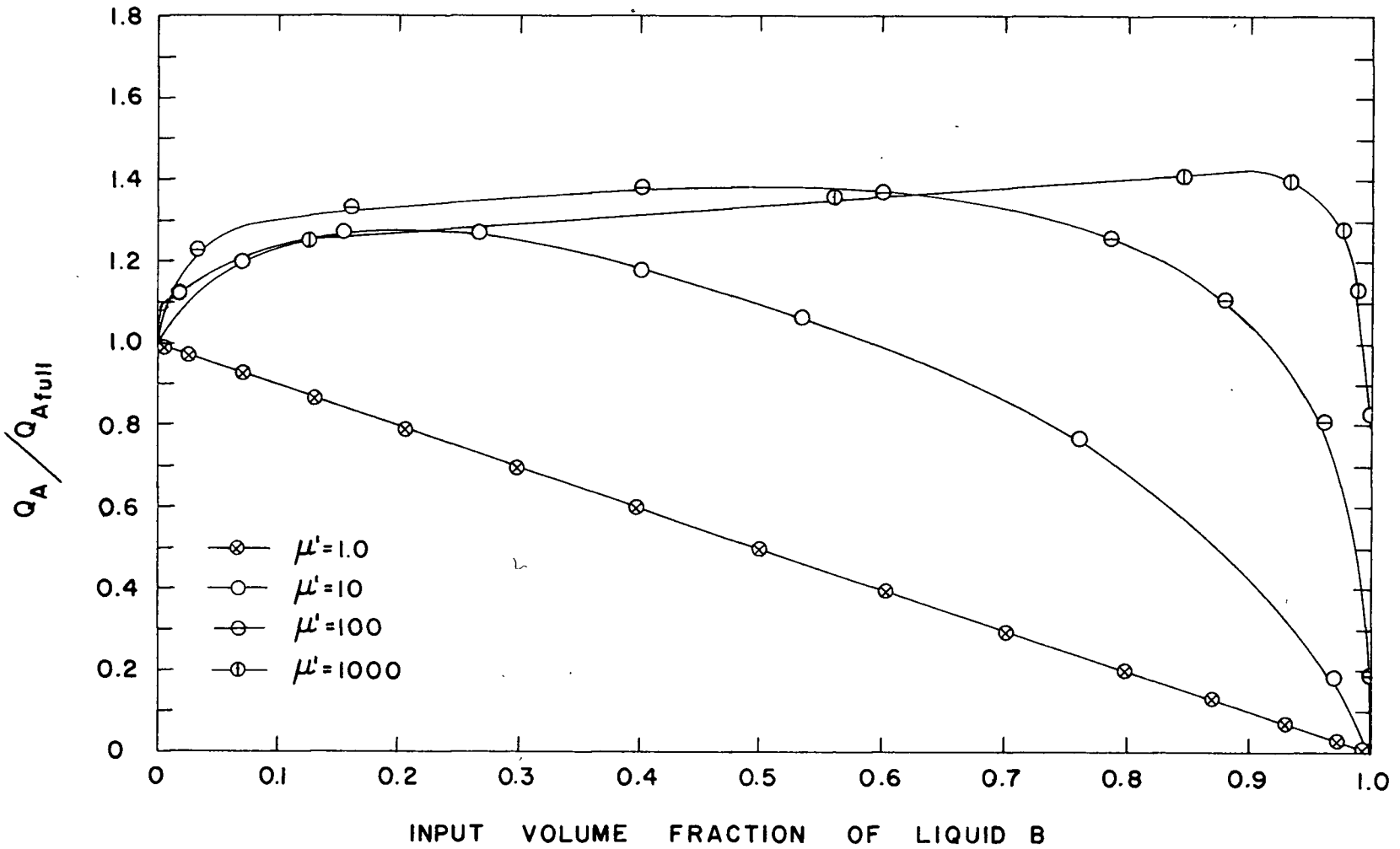

Figure 20. Variation of Volumetric Flow Rate Factor with Input Volume Fraction

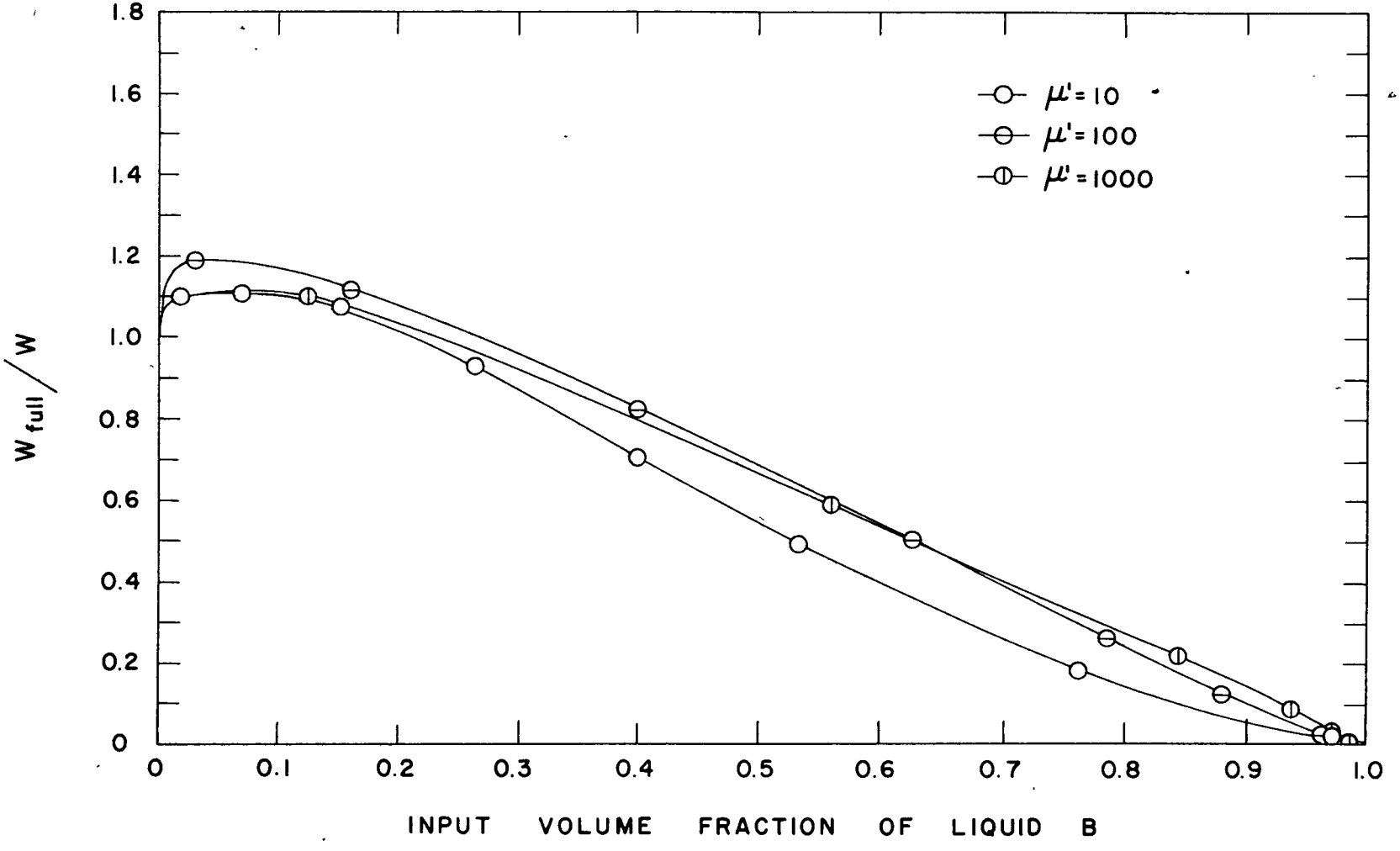

Figure 21. Variation of Power Reduction Factor with Input Volume Fraction

DISCUSSION OF RESULTS

The numerical flow equations were checked by two methods. Comparison of point velocities calculated by relaxation methods with those calculated using Poiseuille's equation, for single-liquid flow, show an average deviation of 1.23% for a numerical solution with unbalanced residuals, and 0.45% for a numerical solution with balanced residuals. Finite difference equations were derived for stratified laminar flow between parallel plates, in a manner similar to those derived in the present study. Velocities determined numerically using these equations were compared to velocities calculated analytically (2), for the case of an interface located mid-way between the two plates and a viscosity ratio of 1000. Corresponding velocities were identical. These comparisons show that the numerical method of solution employed is accurate.

The velocity profiles computed numerically for the round pipe were consistent with those calculated analytically for parallel plates. As the viscosity ratio increased, the point velocities of the less viscous liquid B, as compared to the point velocities of the more viscous liquid A, increased approximately to the same degree as the viscosity ratio. This result can be seen in figure 11.

For a solution with unbalanced residuals, a deviation of 0.64% resulted between the volumetric flow rate calculated by the numerical method and that calculated by Poiseuille's equation, for single-liquid flow. When the residuals were balanced, the deviation could not be detected within three-figure accuracy. This result again shows good agreement between the numerical and analytical solutions.

The volumetric flow rate factor at any specific interface position increased with increasing viscosity ratio. This trend was also followed by the maximum volumetric flow rate factor, as seen in figure 15. From the point of view of volumetric flow rate enhancement, the viscosity ratio of 1000 is practically equivalent to an infinite viscosity ratio. This arises from the fact that equations (18),(19) and (20) produce a constant dimensionless velocity profile, within three-figure accuracy, in liquid A for viscosity ratios greater than 1000. It follows that $\frac{Q_A}{Q_{A\,full}}$ will not increase significantly with an increase of the viscosity ratio above 1000; that is, its value at $\mu' = 1000$ will be within 0.1% of its asymptotic value at infinite μ'. Similar asymptotic behaviour is displayed by the concentric flow model, where the factor $(\mu_A + \mu_B)$ is safely taken as μ_A at viscosity ratios equal to or exceeding 1000 (2).

The interface position of the maximum volumetric flow rate factor moved closer to the bottom of the pipe as

the viscosity ratio increased in the range of 10 to 1000. This is seen in Table VI and figure 13. As can be seen in figures 15 and 20, the input volume fraction of the less viscous liquid increased with increasing viscosity ratio, for the conditions of maximum volumetric flow rate enhancement. In the case of the viscosity ratio of 1000, the maximum enhancement factor is achieved at an input of 81% of liquid B, compared to 8.0% B at a viscosity ratio of 10.

For specific viscosity ratios, the maximum volumetric flow rate factors for stratified flow in a circular pipe were smaller than those for stratified flow between parallel plates, and were very much smaller than those obtained for concentric flow in a circular pipe. This is seen in figure 22 for a viscosity ratio of 10.

The largest of the three computed maximum power reduction factors occured for the case of μ' = 100. The maximum factor for μ' = 10 was slightly larger than that for μ' = 1000. This is easily seen in figures 16, 17 and 18. The case of μ' = 1000 resulted in a lowered power reduction factor because for this case a large input of liquid B, which even occurs at small fractional flow areas, more than counteracts the effect of the lowered pressure gradient at a given throughput of liquid A. The fact that power reduction factors were always lower than corresponding pressure reduction factors can be attributed to the mere presence of B,

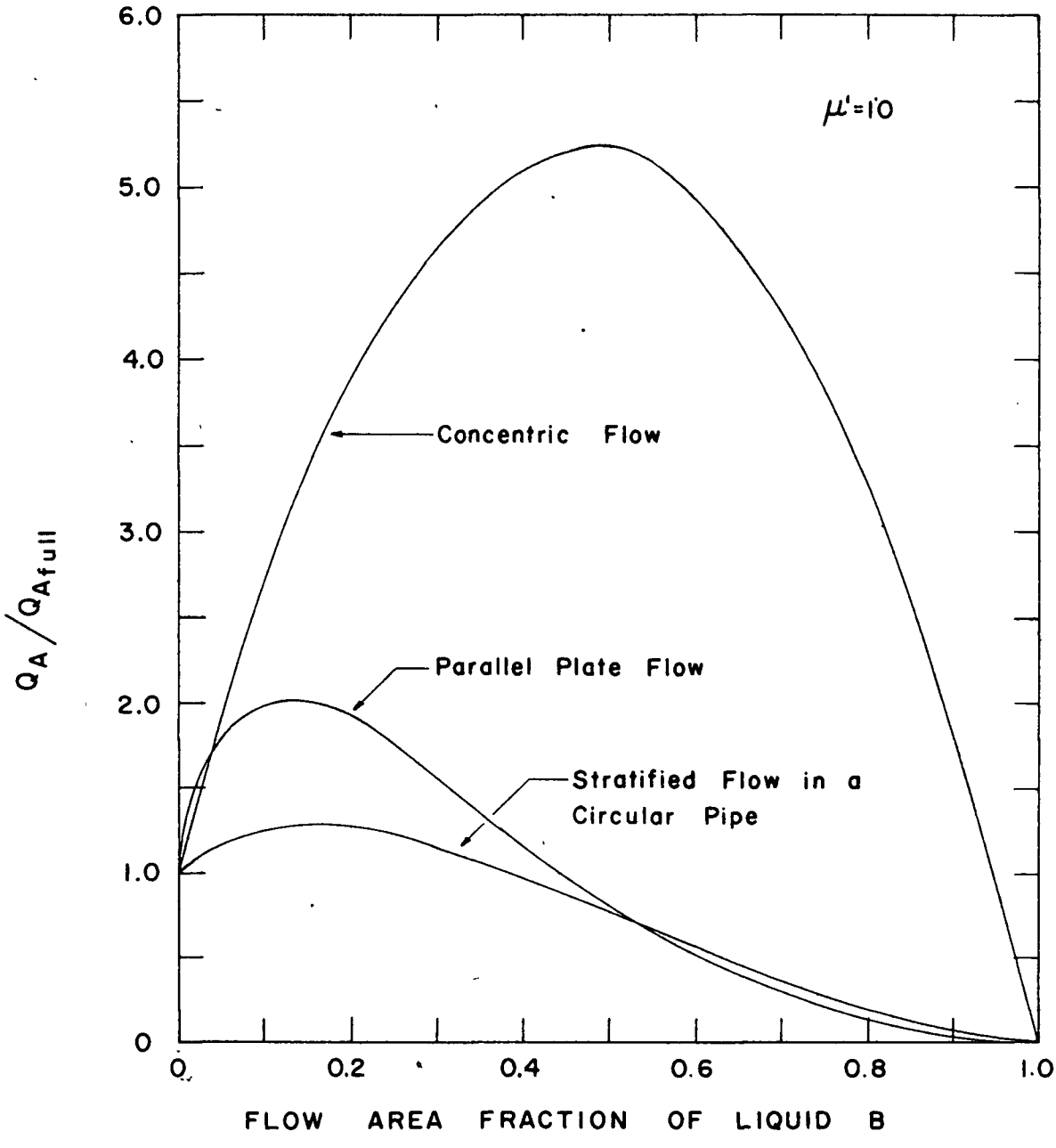

Figure 22. Comparison of Volumetric Flow Rate Factors for Concentric Flow, Parallel Plate Flow and Stratified Flow in a Circular Pipe

which must be incorporated into the calculation of power.

The position of the interface for the maximum power reduction factor moved closer to the bottom of the pipe as the viscosity ratio increased in the region of 10 to 1000. This is seen in Table VIII and figure 16. Over the same range, though, the input volume fraction of liquid B remained essentially constant, with approximately 6.0 to 8.0% of liquid B required to produce the maximum power reduction factor, as seen in figure 18.

In the laminar region, hold-up ratio is a function of input volume ratio and viscosity ratio only. At a constant input volume ratio, the hold-up ratio decreased with increasing viscosity ratios.

An oral presentation on the same topic by Redberger and Charles (12) came to the present author's attention after completion of his calculations. Though the two studies are very similar, a number of differences exist which can be noted here. Redberger and Charles solved the flow equations on an electronic computer, which necessitated that the pipe wall be approximated by horizontal and vertical straight lines. The present calculations were performed using a true circular boundary, negative values being obtained by extrapolation for grid points lying outside the pipe wall. They performed relaxations at the liquid interface in one-dimension only, while the present study incorporated a two-dimensional

relaxation method, necessitated by the velocity variation along the interface. The volumetric flow rate factors calculated here are slightly larger than those calculated by Redberger and Charles, but these authors admit that their results may be conservative. Finally, their calculations were performed for specific pipe diameters and viscosities of the two phases rather than for the general case, as in the present investigation.

COMPARISON OF EXPERIMENTAL AND THEORETICAL RESULTS

A. Experimental Data

The theoretical results of this study were compared to the experimental results reported by Russell, Hodgson and Govier (6). The complete tabular data of their investigations are deposited with the American Documentation Institute (7). Their tests were conducted at 77°F in a horizontal, smooth, transparent pipe, 28.18 feet in length, with an inside diameter of 0.8057 inches. The two liquids used were a refined mineral oil with a specific gravity of 0.834 and a viscosity of 18 c.p., and water with a viscosity of 0.894 c.p., giving a viscosity ratio of 20.1. The two-phase flow was studied at thirteen superficial water velocities and input oil-water volume ratios within the range 0.1-10. These flow rates corresponded to superficial Reynolds numbers ranging from 809 to 24,700 for the water flow and 9.58 to 942 for the oil flow.

Russell et al measured pressure drop in all of their runs and hold-up in some. Most of the pressure drop measurements were made for the whole pipe length, but some were performed on a half-section of pipe.

Lockhart and Martinelli (13) have proposed criteria

for defining the regions of laminar flow and turbulent flow of two cocurrent phases. If the superficial Reynolds number of a phase is less than 1000, the liquid flow is postulated to be laminar, while for superficial Reynolds numbers greater than 2000, the flow is taken as turbulent. The exact point of transition is not known; the criterion of Re = 2000 for turbulence is considered a conservative one. Values of Reynolds numbers between 1000 and 2000 can be considered to be in the transition region. Of the thirteen superficial water velocities studied, only the lowest velocity of 0.116 feet/sec. corresponds to a Reynolds number less than 1000, and is thus in the laminar region. The next four higher water velocities lie in the transition region and the remainder are in the range of turbulent flow. All the oil flow rates investigated were in the laminar region, the largest oil Reynolds number being 942. Therefore, in comparing the theoretical and experimental data, the flow regime must be considered, since all the present theoretical results are based on laminar flow of both liquids.

B. Hold-Up

a. Computational Procedure

A plot of hold-up ratio versus input volume ratio is shown in figure 19 for viscosity ratios of 1, 10, 100 and 1000. From this graph, a cross-plot of hold-up ratio versus viscosity ratio, with input volume ratio as the parameter was drawn. Values for the viscosity ratio of 20.1 were read from the cross-plot, and the theoretical curve of hold-up ratio versus input volume ratio was drawn for $\mu' = 20.1$. This curve was compared to the experimental results by directly plotting on the same graph the corresponding tabular data (7) of Russell, Hodgson and Govier.

b. Results

The cross-plot of hold-up ratio versus viscosity ratio, with input volume ratio as the parameter, is shown in figure 23. From this graph, the theoretical curve of hold-up ratio versus input volume ratio for a viscosity ratio of 20.1 was drawn, as illustrated in figure 24. The experimental results were plotted on the same graph for the eight superficial water velocities for which hold-up data were reported.

c. Discussion of Results

The best agreement between the theoretical and experimental results occurs for the superficial water velocity

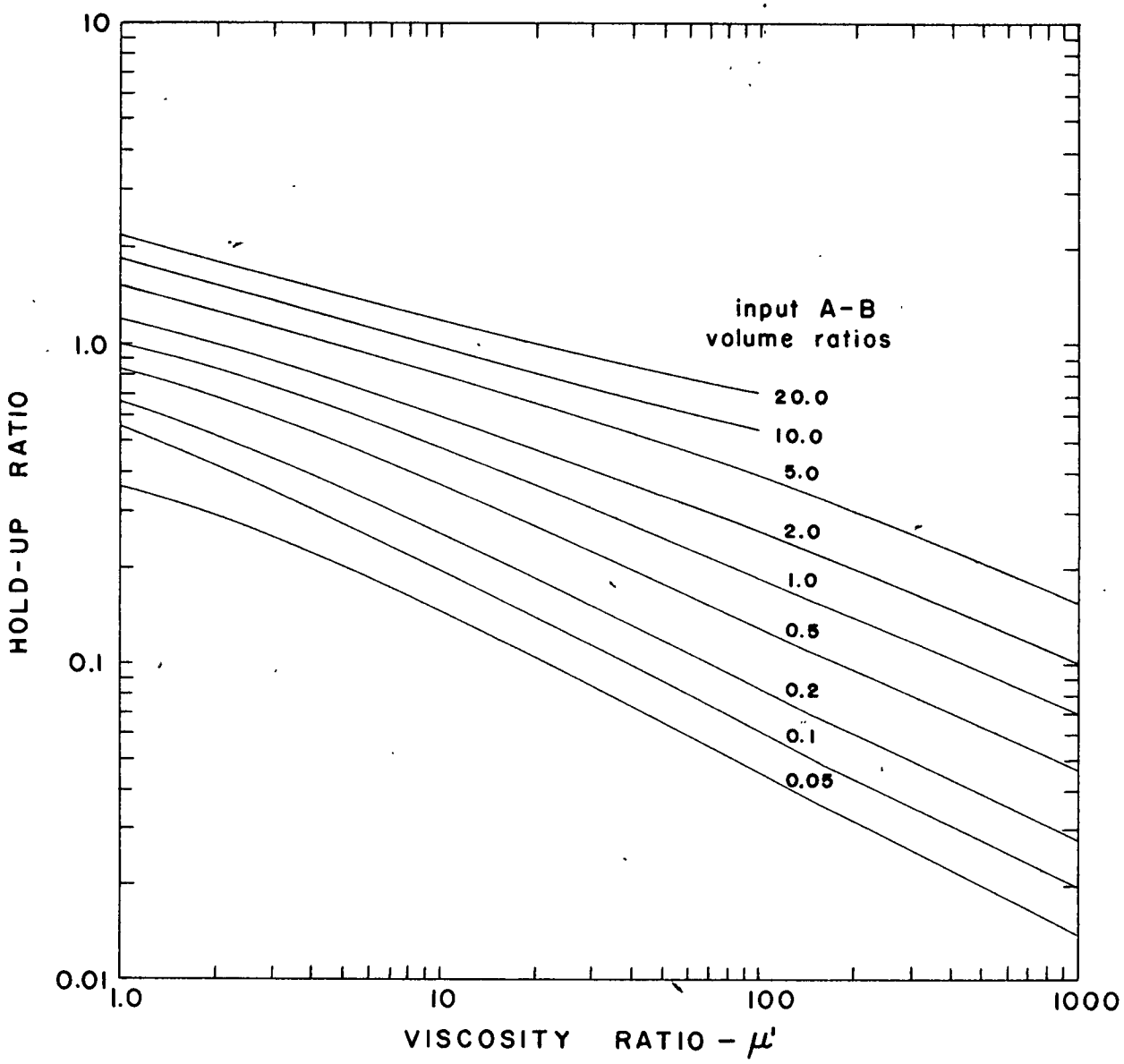

Figure 23. Hold-up Ratio Cross Plot

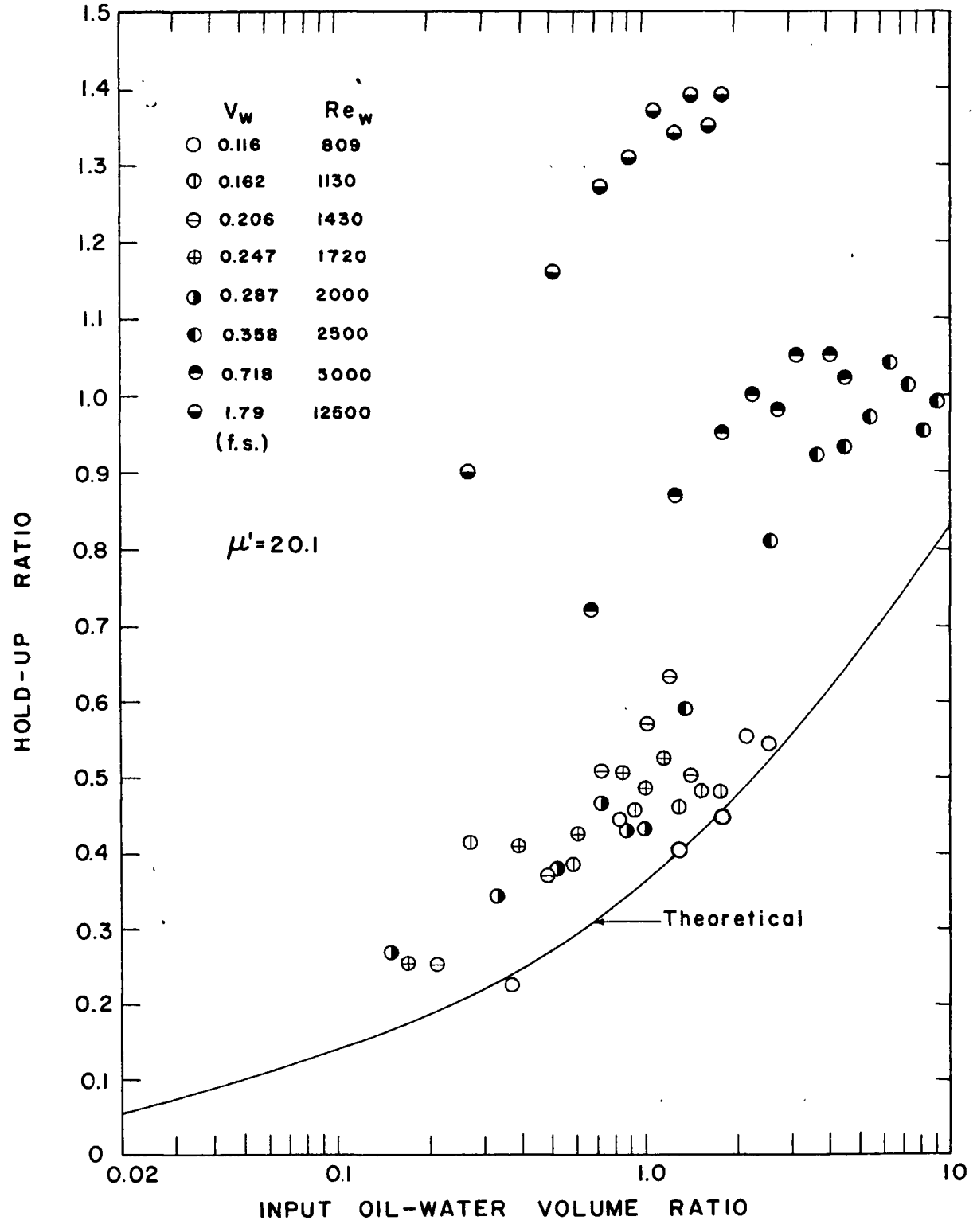

Figure 24. Theoretical and Experimental Hold-up Ratio for μ' = 20.1

of 0.116 ft./sec., corresponding to a Reynolds number of 809. This is the only water flow rate that lies within the laminar region defined by Lockhart and Martinelli (13). Four of the six points for this velocity lie on or very close to the theoretical curve. As the water velocities increase, the agreement between the theoretical and experimental results decreases. This is true even of the data for the four superficial water velocities which fall within the transition region of Re = 1000-2000. These points lie increasingly above the theoretical curve. The data for the three superficial water velocities of 0.358, 0.718 and 1.79 ft./sec., corresponding to Reynolds numbers of 2500, 5000 and 12500 respectively, deviate even more greatly from the theoretical curve, the largest superficial water velocity having the greatest deviation from the theoretical. All three velocities are well within the region of turbulent flow.

From the comparison, it is easily seen that there is close agreement between the experimental and theoretical results in the laminar region. As the flow becomes increasingly turbulent, however, the experimental hold-up ratio develops an increasing positive deviation from the theoretical laminar curve. The hold-up ratio is then no longer a function of input volume ratio and viscosity ratio alone.

C. Pressure Drop

a. Computational Procedure

In order to compare theoretical and experimental pressure drop data, the theoretical values were transformed to dimensional quantities and compared with the experimental points at specific superficial water velocities.

A plot of Q_A/Q_{Afull} versus flow area fraction for $\mu' = 20.1$ was obtained as the first step of the calculations. From figure 13, a cross-plot was made of Q_A/Q_{Afull} versus viscosity ratio, with the interface position as the parameter. From this cross-plot, values of Q_A/Q_{Afull} for $\mu' = 20.1$ were easily obtained for all the interface positions. The interface was expressed in terms of a flow area fraction, as in Appendix II, and the required plot of Q_A/Q_{Afull} versus flow area fraction was then drawn.

The second step in the calculations started with the assumption of a series of input volume ratios. The pressure drop was calculated for each input volume ratio separately. From figure 24, which is a plot of hold-up ratio versus input volume ratio for $\mu' = 20.1$, the hold-up ratio was found for each assumed input volume ratio. Since the in-situ volume ratio is equal to the input volume ratio divided by the hold-up ratio, it was possible to compute the flow area fraction by the relation that

$$\text{flow area fraction} = \frac{\text{in-situ volume ratio}}{1 + \text{in-situ volume ratio}} \qquad (40)$$

Knowing the flow area fraction for an assumed input volume ratio, the value of Q_A/Q_{Afull} at $\mu' = 20.1$ was easily read from the graph determined in the first step of the calculations.

The third step consisted of choosing a superficial velocity of liquid B which is equal to one of the superficial water velocities reported in the experimental paper. The volumetric flow rate of the less viscous liquid, Q_B, is equal to the product of its superficial velocity and the total cross-sectional area of the pipe. The volumetric flow rate of the more viscous liquid, Q_A, is given as

$$Q_A = Q_B \text{ (input volume ratio)} \qquad (41)$$

and

$$Q_{Afull} = Q_A \Big/ \frac{Q_A}{Q_{Afull}} \qquad (42)$$

From the Poiseuille equation,

$$\left(-\frac{\Delta P}{L}\right) = \frac{128 \mu_A Q_{Afull}}{\pi g_c D^4} \qquad (43)$$

All the values on the right hand side of equation (43) were then known. Therefore $\left(-\frac{\Delta P}{L}\right)$ could be calculated for an assumed input volume ratio, for a chosen superficial velocity. The calculations were repeated for the several input volume ratios assumed, and a theoretical curve of pressure drop versus input volume ratio was thus drawn for the given

superficial water velocity. This procedure was repeated for the other twelve water rates. The experimental data were converted to the same units as the theoretical, and were plotted with the theoretical curves.

b. Sample Calculations and Results

The cross-plots of Q_A/Q_{Afull} versus viscosity ratio, with interface position as the parameter, are shown in figure 25. From these plots, values of Q_A/Q_{Afull} for μ' = 20.1 were obtained for various interface positions. Having expressed the interface position in terms of flow area fraction as in Table X, Appendix II, Q_A/Q_{Afull} was plotted against flow area fraction for μ' = 20.1, as illustrated in figure 26.

Assume an input A-B volume ratio = 5.00

From figure 24, the hold-up ratio = 0.655

Therefore the in-situ volume ratio = $\frac{5.00}{0.655}$ = 7.63

and the flow area fraction of A = $\frac{7.63}{8.63}$ = 0.884

From figure 26, Q_A/Q_{Afull} = 1.31

Choose superficial water velocity of liquid B = 0.116 ft./sec.

Diameter of pipe = 0.8057 in. = 0.0671 feet.

Area of pipe = $\frac{(0.8057)^2}{4x144}$ = 0.00354 ft.^{2}

Therefore Q_B = (0.116)(0.00354) = 0.000411 ft.^{3}/sec.,

Q_A = (0.000411)(5.00) = 0.00206 ft.^{3}/sec.,

and $Q_{Afull} = \frac{0.00206}{1.31}$ = 0.00157 ft.^{3}/sec.

Now μ_A = 0.0121 lbs./ft.sec.

and g_c = 32.174 poundals/lt.-force

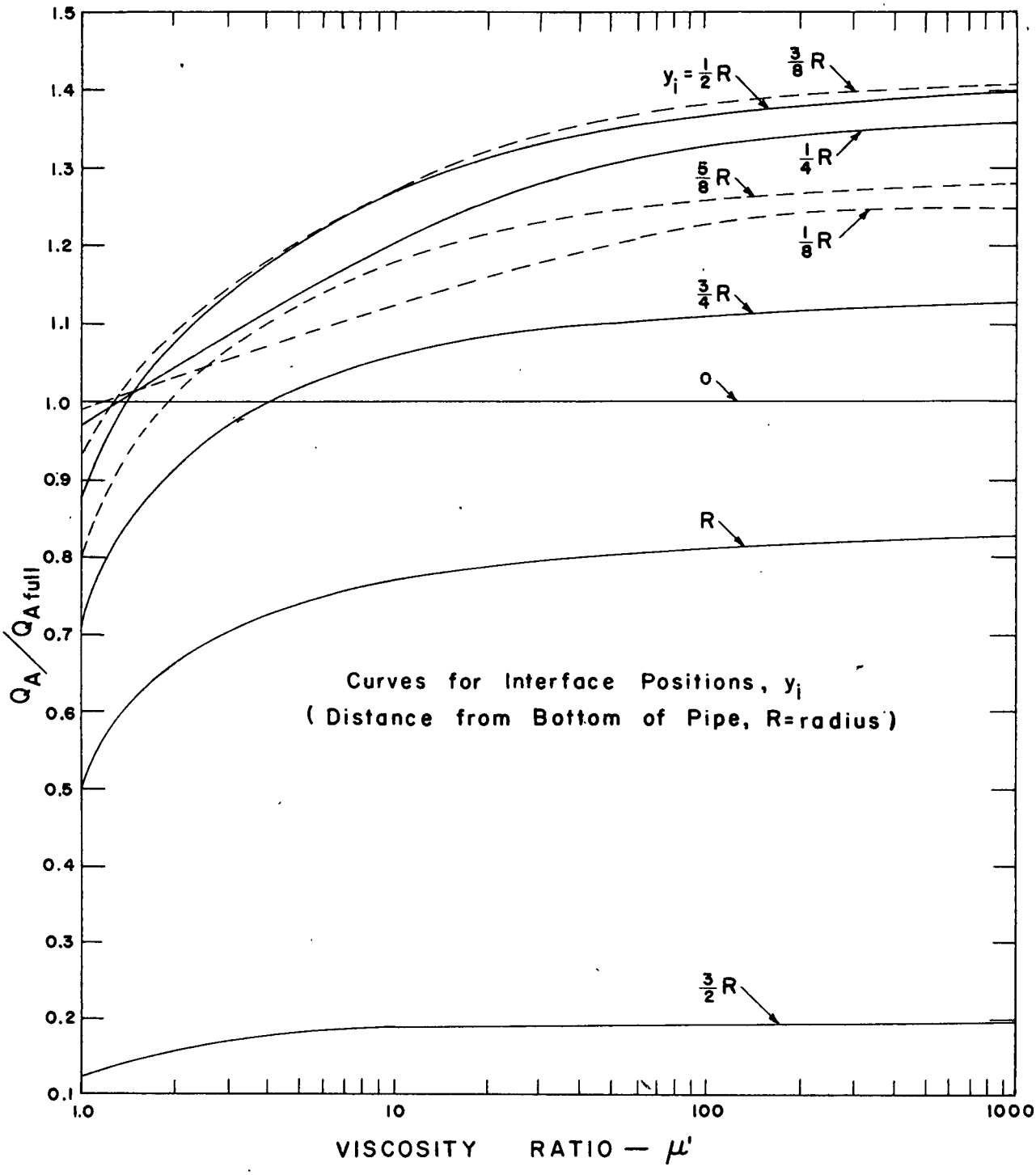

Figure 25. Variation of Volumetric Flow Rate Factor with Viscosity Ratio

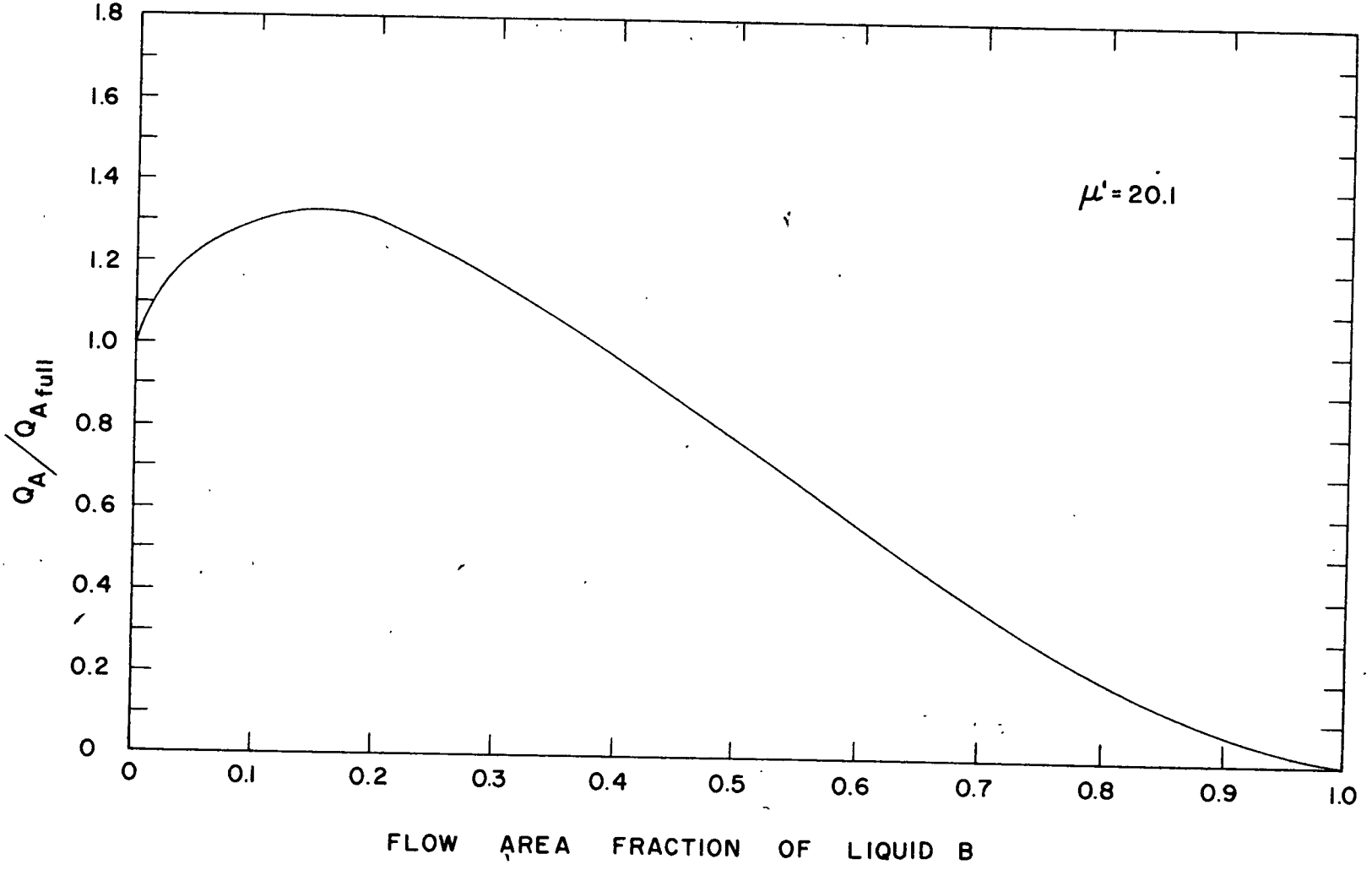

Figure 26. Variation of Volumetric Flow Rate Factor with Flow Area Fraction for $\mu' = 20.1$

Therefore $(-\frac{\Delta P}{L}) = \frac{128(0.0121)(0.00157)}{\pi(32.174)(0.0671)^4} = 1.19$ lbs./ft.^{2}/ft.

This calculation was repeated for several input volume ratios, so that the theoretical curve could be obtained.

Data for a typical experimental point are as follows:

Superficial water velocity = 0.116 ft./sec.

Experimental input oil-water volume ratio = 4.21

Average pressure drop = 6.90 inches of water

$= (6.90)(5.202) = 35.9$ lbs./ft.^{2}

Length of test section = 28.18 feet

and therefore pressure gradient $(-\frac{\Delta P}{L}) = \frac{35.9}{28.18} = 1.27$ lbs./ft.^{2}/ft.

This tabulation was repeated for all the input oil-water volume ratios reported, and the experimental results were plotted on the same graph as the theoretical curve.

The theoretical curves and experimental data for the thirteen water rates were plotted in figures 27, 28, and 29 as pressure gradient versus input volume fraction.

c. Discussion of Results

In figure 27, experimental data are shown for the superficial water velocity of 0.116 ft./sec., Re = 809. This is the only water flow rate which definitely lies within the laminar region, and the experimental and theoretical results show very close agreement for this case. The data for the

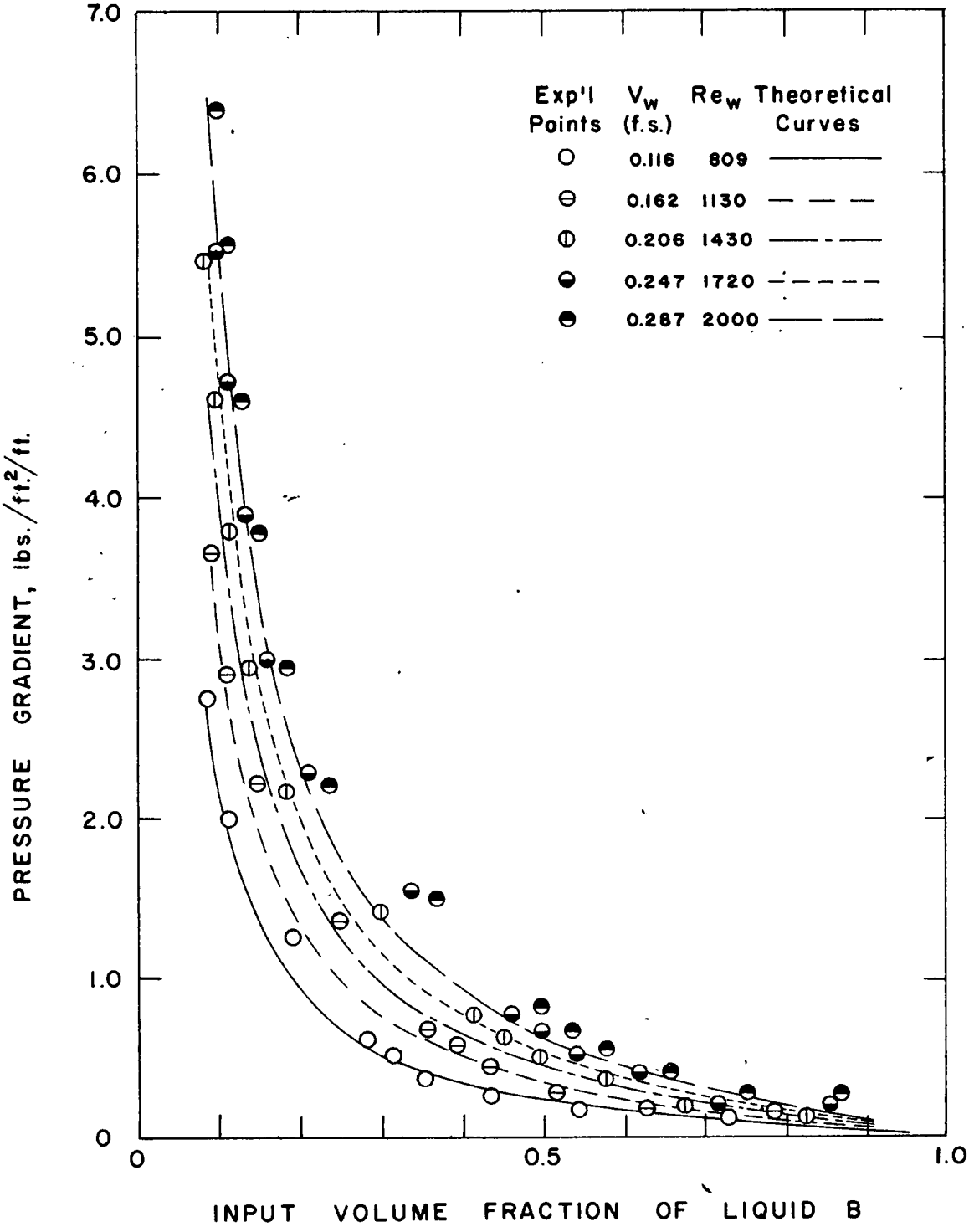

Figure 27. Theoretical and Experimental Pressure Gradients for V_w = 0.116 - 0.287 f.s.

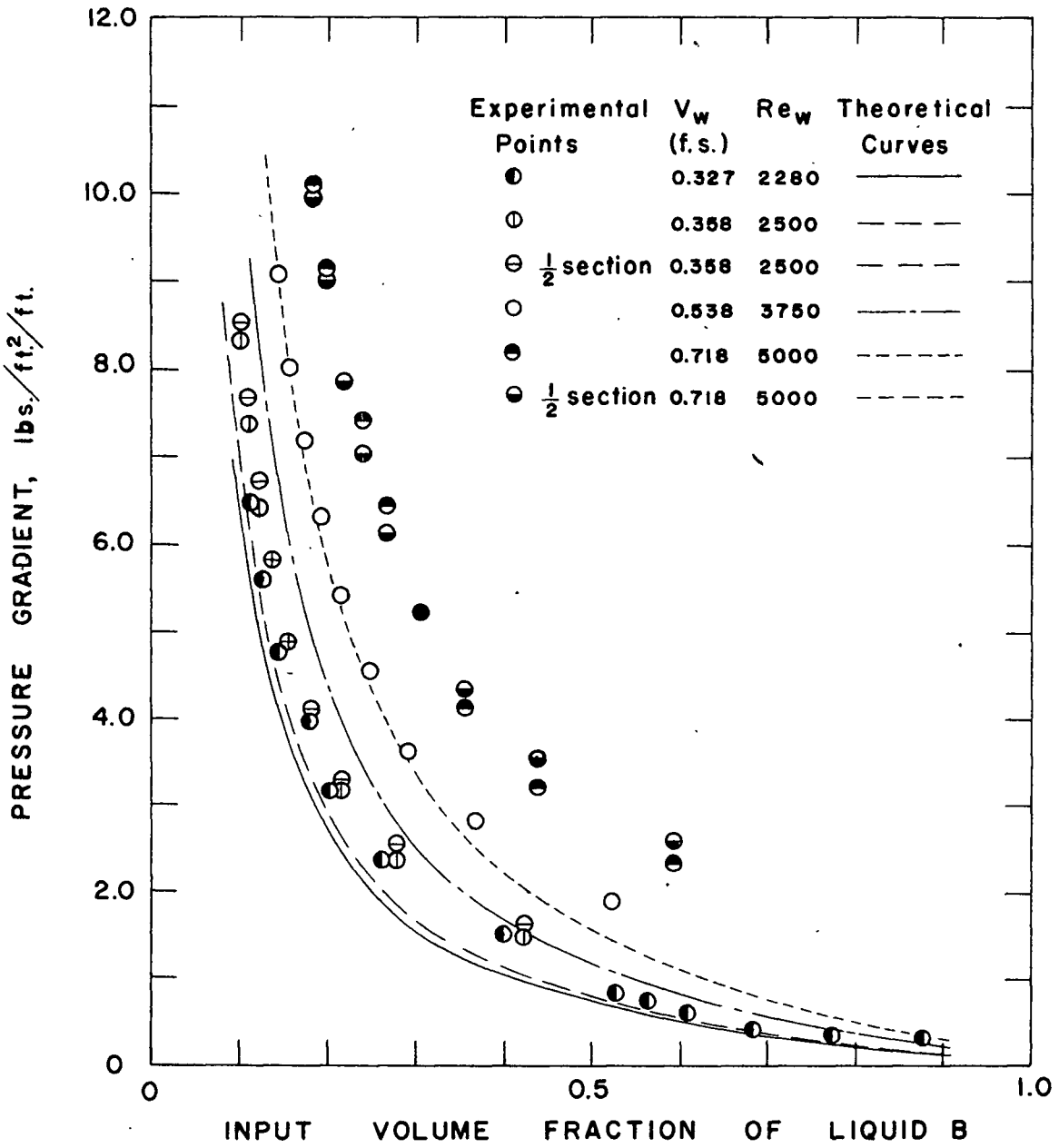

Figure 28. Theoretical and Experimental Pressure Gradients for V_w = 0.327 - 0.718 f.s.

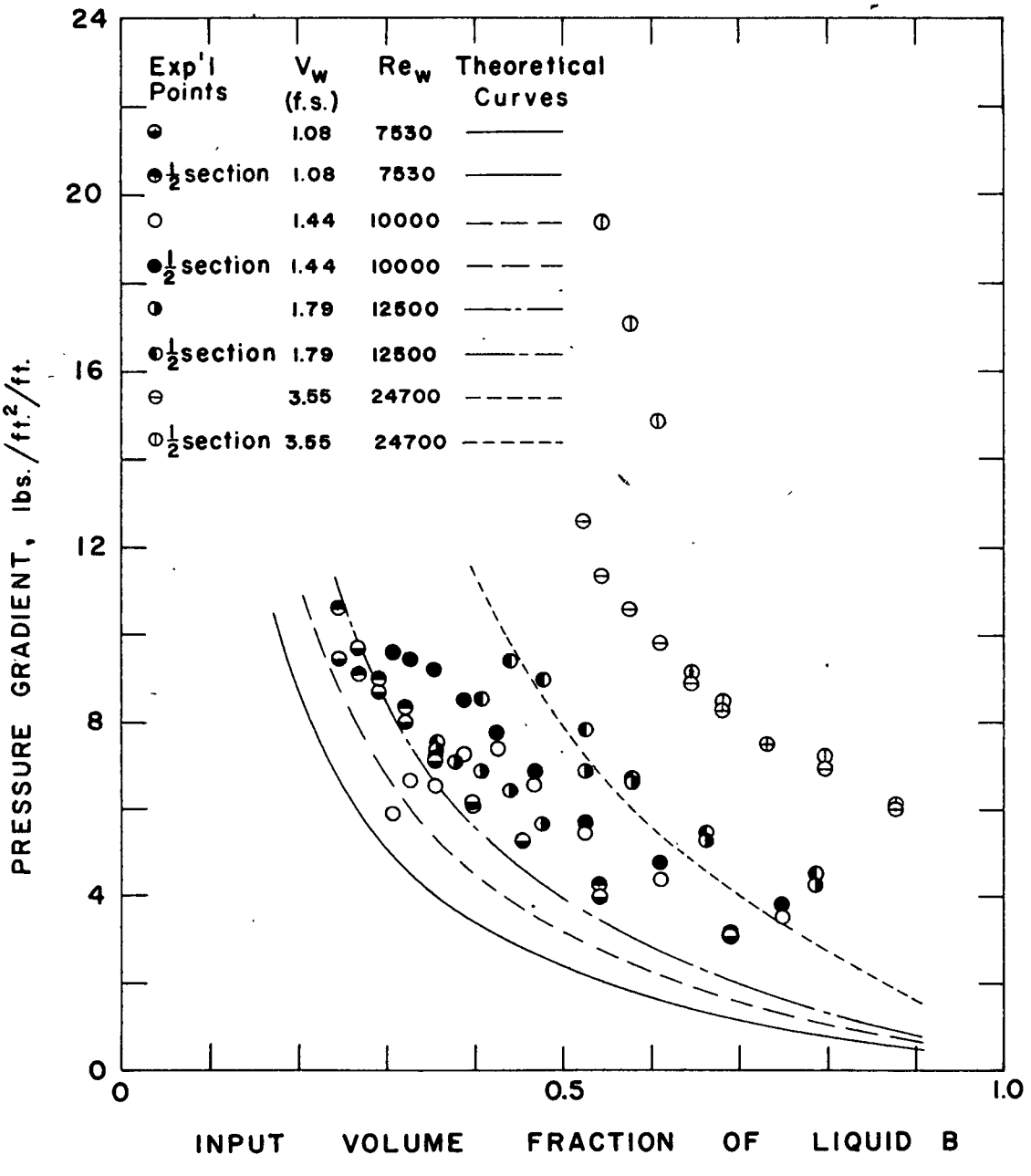

Figure 29. Theoretical and Experimental Pressure Gradients for V_w = 1.08 - 3.55 f.s.

other four velocities plotted in figure 27 lie in the transitional region, and it is seen that agreement between the experimental and theoretical results is not quite as good.

Figures 28 and 29 contain experimental data for flow rates which all lie in the turbulent region, and they show increasing deviation from the theoretical curve as the velocity increases. At the highest superficial water velocity of 3.55 ft./sec., the deviation is very great.

Therefore the experimental and theoretical results agree in the laminar region, but as turbulence increases, the agreement decreases. In the turbulent region, the experimental pressure drops are very much greater than those predicted theoretically for laminar flow. This disagreement is in the anticipated direction.

D. Enhancement of Volumetric Flow Rate

a. Computational Procedure

The comparison of experimental and theoretical volumetric flow rate factors was made on a plot of Q_A/Q_{Afull} versus input volume fraction of liquid B. The input volume fraction was chosen because it gives a better representation of the data than input volume ratio.

Figure 24 is a plot of hold-up ratio versus input A-B volume ratio for $\mu' = 20.1$. From this figure, the in-situ A-B volume ratio for a corresponding input A-B volume ratio was determined, knowing that the hold-up ratio is equal to the input volume ratio divided by the in-situ volume ratio. The flow area fraction of liquid B was calculated from the in-situ A-B volume ratio, and from figure 26 the corresponding value of Q_A/Q_{Afull} was obtained. In this way the entire theoretical curve of Q_A/Q_{Afull} versus input volume fraction of liquid B was plotted.

The experimental input oil-water volume ratio was converted to the input volume fraction of water as follows:

$$\text{input volume fraction of water} = 1-\frac{\text{input oil-water volume ratio}}{1+\text{input oil-water volume ratio}} \qquad (44)$$

Previously it was proved that

$$\frac{\left(-\frac{\partial P}{\partial x}\right)_{full}}{\left(-\frac{\partial P}{\partial x}\right)} \text{ at constant } Q_A = \frac{Q_A}{Q_{Afull}} \text{ at constant } \left(-\frac{\partial P}{\partial x}\right) \quad (28)$$

Therefore if the experimental pressure reduction factor could be calculated, it would be equal to the volumetric flow rate enhancement factor. The ratio of the pressure gradient for the pipe flowing full of oil to the measured experimental pressure gradient for two-phase flow was expressed as

$$\frac{\left(-\frac{\partial P}{\partial x}\right)_{full}}{\left(-\frac{\partial P}{\partial x}\right)_{exp.}} = \frac{-\frac{32\mu_{oil}V_{oil}}{g_c D^2}}{\left(-\frac{\partial P}{\partial x}\right)_{exp.}} \quad (45)$$

The superficial oil velocity was calculated as

$$V_{oil} = V_{water} \text{ (input volume ratio)} \quad (46)$$

and then all the values on the right hand side of equation (45) were known. Thus the experimental pressure gradient factor or its equivalent, the volumetric flow rate factor, were calculated for all the experimental data, and these were plotted on the same graph as the theoretical curve.

b. Sample Calculations and Results

Consider first the theoretical calculations.

Assume an input A-B volume ratio = 5.00

From figure 24, hold-up ratio = 0.655

Therefore in-situ A-B volume ratio = $\frac{5.00}{0.655}$ = 7.63

and the flow area fraction of liquid B = $1-\frac{7.63}{8.63}$ = 0.116

From figure 26, Q_A/Q_{Afull} = 1.31

Corresponding input volume fraction of liquid B =

$$1 - \frac{5.00}{6.00} = 0.167$$

This calculation was repeated for various input volume ratios, and a plot of Q_A/Q_{Afull} versus input volume fraction of liquid B is shown in figure 30.

Now consider the experimental data.

Superficial water velocity = 0.116 ft./sec.

Input oil-water volume ratio = 4.21

Superficial oil velocity = (0.116)(4.21) = 0.488 ft./sec.

Oil viscosity = 0.0121 lbs./ft.sec.

= 32.174 poundals/lb.-force

Pipe diameter, D = 0.0671 feet

Therefore $(\frac{\partial P}{\partial x})_{full} = \frac{32(0.0121)(0.488)}{(32.174)(0.0671)^2}$ = 1.30 lbs./ft.^{2}/ft.

From the previous section

$$(\frac{\partial P}{\partial x})_{exp.} = 1.27 \text{ lbs./ft.}^2\text{/ft.}$$

Hence $\frac{Q_A}{Q_{Afull}} = \frac{1.30}{1.27} = 1.02$

and the input volume fraction of water = $1 - \frac{4.21}{5.21}$ = 0.192

The experimental data for all thirteen superficial water velocities are plotted in figure 30.

LEGEND FOR FIGURE 30

(On reverse side)

LEGEND FOR FIGURE 30

Experimental Points		Vw (f.s.)	Re_w
○		0.116	809
⊙		0.162	1130
⊖		0.206	1430
⊕		0.247	1720
⊗		0.287	2000
⊗		0.327	2280
◓		0.358	2500
◒	½ section	0.358	2500
●		0.538	3750
◐		0.718	5000
◑	½ section	0.718	5000
◫		1.08	7530
⊟	½ section	1.08	7530
▧		1.44	10000
▨	½ section	1.44	10000
◧		1.79	12500
◨	½ section	1.79	12500
▬		3.55	24700
▬	½ section	3.55	24700

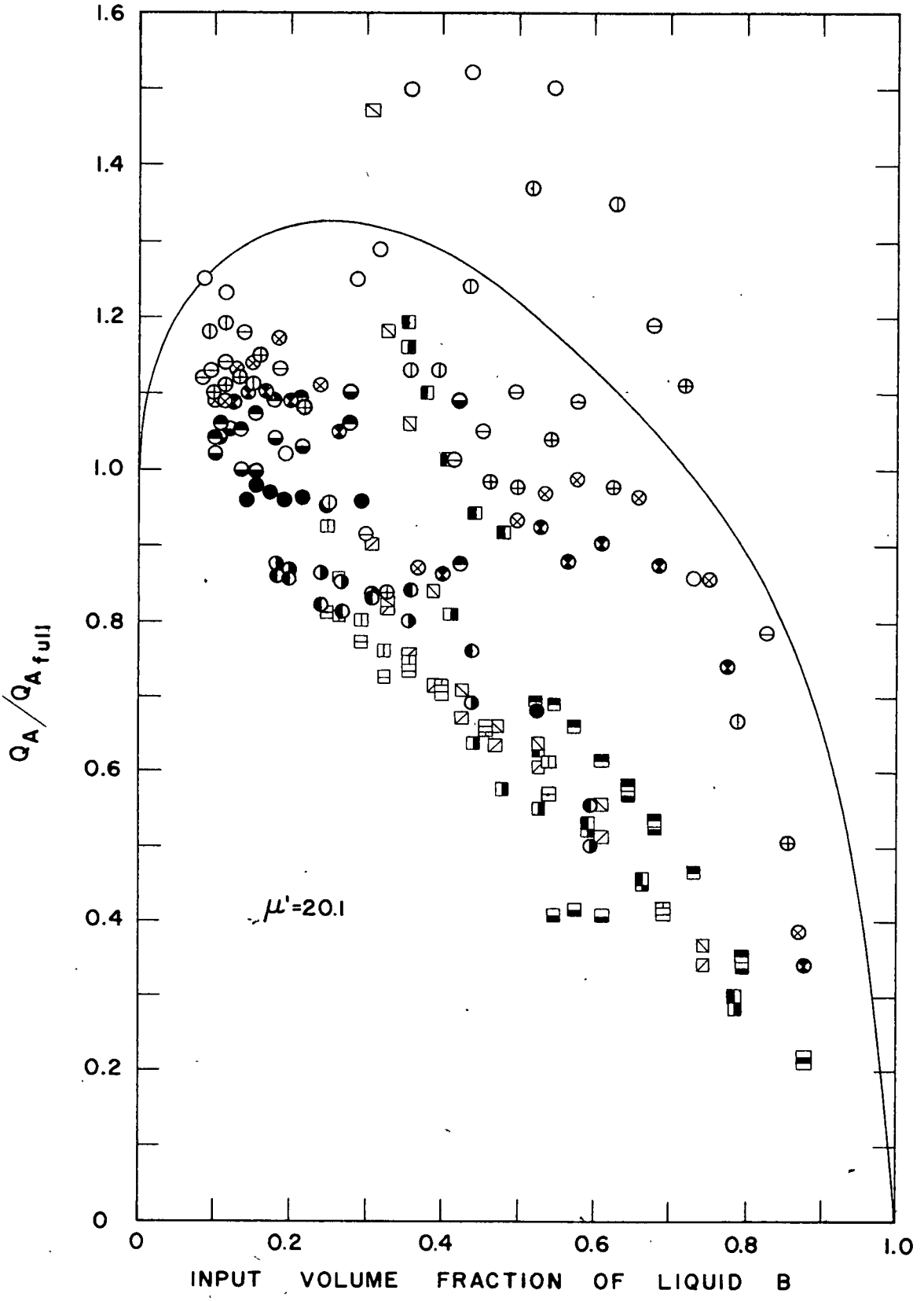

Figure 30. Theoretical and Experimental Volumetric Flow Rate Factors for μ' = 20.1

c. Discussion of Results

The experimental results in figure 30 show a wide scatter of points. A trend is noted, though, that the values of the volumetric flow rate factor in the turbulent region lie much lower than the theoretical curve and that values in the laminar and transitional regions are closer to the theoretical curve. A few experimental points even fall above the theoretical curve, and it is therefore presumed that perfect horizontal stratification did not necessarily occur but that the interface may have been slightly curved. Such a slight tendency towards concentric flow would result in raising the volumetric flow rate factor (see figure 22).

Russell et al (2,6) reported a pressure gradient reduction factor of 1.2 for 10% water input, and it is seen that this agrees with the experimental values plotted in figure 30. Later they reported this as their maximum factor, but it is seen in figure 30 that factors greater than 1.2 were actually obtained, as was mentioned in the introduction.

CONCLUSIONS

Theoretical volumetric flow rate enhancement factors, power reduction factors and hold-up ratios have been derived numerically for the stratified laminar flow of two immiscible Newtonian liquids flowing in a circular pipe, for viscosity ratios of the two liquids ranging from 1 to 1000, and for various positions of the liquid-liquid interface.

The volumetric flow rate enhancement factor at any specific interface position increases with increasing viscosity ratio. A similar trend is also followed by the maximum volumetric flow rate factor which achieves a maximum asymptotic value at infinite viscosity ratio. This asymptotic value is practically reached at a viscosity ratio of 1000.

For the range of viscosity ratio from 10 to 1000, the position of the interface for the maximum volumetric flow rate factor moves closer to the bottom of the pipe with increasing viscosity ratio. However, the input volume fraction of the less viscous liquid, for the condition of maximum volumetric flow rate enhancement of the more viscous liquid, increases with increasing viscosity ratio.

At specific viscosity ratios, the maximum volumetric flow rate factor for stratified flow in a

circular pipe is smaller than the corresponding maximum factor for parallel plate flow, and very much smaller than the corresponding maximum factor for concentric flow in a circular pipe.

Power reduction factors are always lower than corresponding volumetric flow rate factors.

The position of the interface for the maximum power reduction factor moves closer to the bottom of the pipe as the viscosity ratio increases in the range of 10 to 1000. In the same range, the input volume fraction of the less viscous liquid necessary to produce the maximum factor remains essentially constant.

For laminar flow of both liquids, hold-up ratio is a function of input volume ratio and viscosity ratio only.

The present theoretical results and the experimental results of Russell, Hodgson and Govier for the case of laminar flow of both phases, show good agreement with regard to hold-up ratios, pressure gradients and volumetric flow rate enhancement factors. In the case of experimental results in the transition region of flow of the less viscous liquid, there is distinct disagreement between these results and the present theoretical laminar flow results. This expected disagreement increases as the flow of the less viscous liquid becomes increasingly turbulent.

The pressure gradient reduction factors measured experimentally for the two crude oils reported in table I fall between the values determined theoretically for concentric flow and stratified flow in a circular pipe. These results substantiate the statement by Russell and Charles that the flow for these experiments was intermediate between the stratified and concentric models.

REFERENCES

1. Clarke, K.A., private communication quoted in reference 2, (1948).

2. Russell, T.W.F., and Charles, M.E., 35, 18 (1959).

3. Clark, A.F., and Shapiro, A., U.S. Patent No. 2,533,878 (May 1949).

4. Chilton, E.G., and Handley, L.R., U.S. Patent No. 2,821,205 (Jan. 1958).

5. Chilton, E.G., C.J.Ch.E., 37, 127 (1959).

6. Russell, T.W.F., Hodgson, G.W., and Govier, G.W., C.J.Ch.E., 35, 9 (1959).

7. Document No. 5772, A.D.I. Auxiliary Publications Project, Photoduplication Service, Library of Congress, Washington, D.C.

8. Tipman, E., and Hodgson, G.W., J. Petrol. Tech. 8, No. 9, 91 (1956).

9. Pavlov, P.P., Trudy Azerbaidzahn, Ind. Inst. im. M. Azizbekova, No. 9, 76 (1955).

10. Mickley, H.S., Sherwood, T.K., and Reed, C.E., Applied Mathematics in Chemical Engineering, 2nd Edition, McGraw-Hill (1957).

11. Allen, D.N. de G., Relaxation Methods, McGraw-Hill (1954).

12. Redberger, P.J. and Charles, M.E., Syposium "Multiphase Flow in the Production and Drilling of Oil Wells", A.I.Ch.E. - S.P.E. Joint Meeting, Tulsa, Oklahoma, Sept. 25-28, 1960.

13. Lockhart, R.W., and Martinelli, R.C., Chem. Eng. Progress, 45, 39 (1949).

14. Perry, J.H., Chemical Engineers Handbook, 3rd Edition, McGraw-Hill (1950).

APPENDIX

I. Relaxation Methods

Relaxation methods can in general be used to solve various types of differential equations, but for this study they were used to solve only linear second order partial differential equations. This section will describe how relaxation methods are employed to solve this particular type of equation.

The partial differential equation representing the flow conditions investigated, is rewritten as a finite difference equation of the form

$$u'_1 + u'_2 + u'_3 + u'_4 - 4u'_o + 8\mu'(\Delta y')^2 = 0 \qquad (16)$$

as shown on page 12a. The above equation suggests that the velocity at the point O is equal to the arithmetric mean of the velocity at four surrounding points, plus a constant. The relative position of the five points referred to are shown in figure 2. Suppose the values of the five velocities were guessed at and substituted in equation (19). If the guesses were incorrect, a remainder or residual would result because the equation would not be satisfied. The residual can be expressed as

$$u'_1 + u'_2 + u'_3 + u'_4 - 4u'_o + 8\mu'(\Delta y')^2 = \text{Residual} \qquad (47)$$

It is noticed that by increasing the value of u'_o by 1, the residual is decreased by 4, whereas increasing the value of any of the surrounding velocities by 1, increases the residual by 1. This 4 to 1 ratio leads to convergence towards the solution, which is attained when the residual is zero or approximately zero. For example, a new guess of u'_o greater than the previous value by one-quarter of the residual, will eliminate the residual and thus achieve a tentative solution.

This procedure is then applied to a grid of points as in figure 5, where all the point velocities are guessed at, and the residuals calculated for each point using equation (19). The point with the largest residual is relaxed first by rendering the residual equal to zero. This procedure is repeated until all the residuals are approximately equal to zero, in which case the desired solution has been arrived at.

There are methods of aiding convergence to the solution, such as over-relaxation and block relaxation, but these are refinements of the basic method described above. Mickley, Sherwood and Reed (10) present a brief description of relaxation methods, its refinements and some examples of its use, but a more complete description is found in Allen's text (11).

II. Flow Area Fraction

The relationship between the interface position and flow area fraction is developed from the expression for the area of a segment of a circle which is

$$\text{Area} = \frac{1}{2} r^2(\Theta - \sin\Theta) \qquad (48)$$

where Θ is the central angle of radian measure and r is the radius. Since $\cos\frac{\Theta}{2} = (r-h)/h$, Perry (14) has expressed this area in terms of the height, h, of the segment (which corresponds to the interface position y_i) and the diameter D of the circle, and presents a table relating the area of the circular segment to the ratio h/D. Thus, knowing the interface position, the area of the segment is easily arrived at. Dividing this area by the total cross-sectional area of the pipe results in the flow area fraction. The following table was determined using this information.

Table X

Interface Position	Flow Area Fraction of Liquid B
0	0
R/8	0.02602
R/4	0.07214
3R/8	0.1298
R/2	0.1955
5R/8	0.2670
3R/4	0.3425
R	0.5000
3R/2	0.8045
2R	1.0000

II. Flow Area Fraction

The relationship between the interface position and flow area fraction is developed from the expression for the area of a segment of a circle which is

$$\text{Area} = \frac{1}{2} R^2(\Theta - \sin\Theta) \qquad (48)$$

where Θ is the central angle of radian measure and R is the radius. Since $\cos\frac{\Theta}{2} = (R-H)/H$, Perry (14) has expressed this area in terms of the height, H, of the segment (which corresponds to the interface position y_i) and the diameter D of the circle, and presents a table relating the area of the circular segment to the ratio H/D. Thus, knowing the interface position, the area of the segment is easily arrived at. Dividing this area by the total cross-sectional area of the pipe results in the flow area fraction. The following table was determined using this information.

Table X

Interface Position y_i	Flow Area Fraction of Liquid B
0	0
R/8	0.02602
R/4	0.07214
3R/8	0.1298
R/2	0.1955
5R/8	0.2670
3R/4	0.3425
R	0.5000
3R/2	0.8045
2R	1.0000

III. Douglass-Avakian Method

The Douglass-Avakian method, which is described by Mickley, Sherwood and Reed (10), employs a fourth degree polynomial which is fitted to seven equidistant points to give the best curve through them. The polynomial is

$$X = a + bZ + cZ^2 + dZ^3 + eZ^4 \tag{49}$$

The seven points must be spaced at equal intervals h of Z, and the coordinates adjusted so that Z = 0, for the central point. The seven values of the variable Z are then -3h, -2h, -h, o, h, 2h and 3h, and k is the coefficient of h in the values of Z. Thus at Z = -3h, k = -3; at Z = -2h, k = -2 etc. The values of the constants are given by the following expressions:

$$a = \frac{524\Sigma X - 245\Sigma k^2X + 21\Sigma k^4X}{924} \tag{50}$$

$$b = \frac{397\Sigma kX}{1512h} - \frac{7\Sigma k^3X}{216h} \tag{51}$$

$$c = \frac{-840\Sigma X + 679\Sigma k^2X - 67\Sigma k^4X}{3168h^2} \tag{52}$$

$$d = \frac{-7\Sigma kX + \Sigma k^3X}{216h^3} \tag{53}$$

$$e = \frac{72\Sigma X - 67\Sigma k^2X + 7\Sigma k^4X}{3168h^4} \tag{54}$$